く影響し，原薬の生物活性にも影響を与える可能性が考えられることから，製品の品質の一定性を確保するためには，PEG あるいは糖など修飾条件，精製工程などは厳密に工程管理されなければならない。また，工程管理の中では，PEG あるいは糖鎖など付加反応に用いられる各種試薬の品質管理なども必要であろう。最終製品の規格および試験方法で不均一性を含む製品の品質特性プロフィール全体をカバーした十分な試験が実施できないときには，修飾条件，精製工程の工程管理や各種試薬の品質管理をより厳密に行うことで総合的に製品の品質とその恒常性を保証する必要がある。

機能性人工タンパク質の生物学的性質に関しては，天然に存在するタンパク質からの構造改変により目的以外の生物活性が変化している可能性があるため，慎重な検討が必要である。改変により意図しない変化が生じた例として，持続型のインスリン改変体であるインスリングラルギンでは，インスリン受容体との親和性はインスリンと差異がないものの，インスリン様成長因子 IGF-1 受容体との結合親和性がインスリンの 6～8 倍であると報告されている[4]。げっ歯類を用いた 24 ヵ月間反復投与の発がん性試験により，インスリングラルギンは発がん性を有さないと判断されているが，IGF-1 受容体への高親和性結合と安全性との関連の全貌が必ずしも明らかにされたとは言えない。このような特性を持つ機能性人工タンパク質で従来の製品より医薬品としてより有用と目されるものの場合には承認を可とされたとしても，市販後安全対策(ファーマコビジランスプランニング)をしっかりとたて，市販後調査などにより安全性を慎重に観察していく必要がある。ちなみに，医薬品として実用化されているものではないが，B 鎖 10 番目の His を Asp に置換し，インスリン受容体との親和性が亢進した改変インスリンでは，ラットで乳腺腫瘍の発生が報告されている[5),6)]。1 アミノ酸の置換により発がん性が生じることを示した典型例であり，改変による生物学的性質の変化が安全性に大きく影響する場合があることを認識する必要がある。

機能性人工タンパク質の免疫原性・抗原性についても注意深い観察が必要である。一般に PEG 化タンパク質の場合には免疫原性・抗原性が減弱すると言われている。一方，アミノ酸置換体などの改変タンパク質の場合に必ず懸念されるのが，免疫原性および抗原性の問題である。タンパク質性医薬品の免疫原性や抗原性は，タンパク質の一次構造上の特徴はもとより，高次構造，製剤中の目的物質の凝集体や製造工程由来不純物，添加剤，あるいは投与経路などにも大きく影響される[7)]。通常のヒト型組換えタンパク質性医薬品でも免疫原性や抗原性が問題になる例があるが[8)]，もともとヒトには存在しない機能性人工タンパク質の場合には，その免疫原性・抗原性により一層の注意を払わねばならない。ただし，がんなどのように宿主の免疫機能が低下している患者への機能性人工タンパク質の適用と，免疫機能が過剰に亢進しているアレルギーやリウマチといった炎症性疾患への適用では，異なった免疫原性・抗原性問題への取組みやその評価基準が必要であると考えられる。またヒトに対する抗原性は一般に動物実験では評価できず，非臨床試験における評価は困難であるため，ヒトでの抗原性の予測についての方法論の確立などが望まれるところであるが，当面は治験中や市販後における注意深い臨床観察がなによりも重要であると考えられる。

5. おわりに

本節では，昨今加速度的に創出されつつある機能性人工タンパク質の品質・安全性評価の観点から，現状と将来展望，課題について論じた。ゲノミクス，トランスクリプトミクスやプロテオミクス，グライコミクス，メタボロミクスといった大規模な網羅的解析および高効率高発現・標的細胞

指向性のある遺伝子導入技術や発現制御技術，特異的評価系などによる個々の遺伝子やタンパク質の機能解析により，疾患の治癒に関わるタンパク質(医薬品シーズ・タンパク質)の探索・同定が進展し，今後益々，機能性人工タンパク質が，種々の難治性疾患に対する有用な治療薬として開発の対象となることが期待される。一方で，ウイルスや細菌のゲノム解析等の進歩も相俟って，より効率よく宿主の免疫機能を活性化したり，メモリー機能を亢進させたりするような新興・再興感染症に対する機能性人工ワクチン(抗原タンパク質)の登場も予想される。機能性人工ワクチンの場合，免疫原性・抗原性そのものが薬効となる一方で，非特異的免疫の活性化や精緻に構築されている生体免疫機構を乱すことによる思わぬ副作用が発現する可能性に十分な注意が必要となる。また，分子特性・品質特性，用法・用量や投与期間など考慮しつつ，必要に応じて上述した機能性人工タンパク質の品質・安全性確保上の課題をクリアする必要があると思われる。

参考文献

1) Kurtzhals P., Schaffer L., Sorensen A., Kristensen C., Jonassen I., Schmid C. and Trub T. : Correlations of receptor binding and metabolic and mitogenic potencies of insulin analogs designed for clinical use. Diabetes, 49 : 999-1005, 2000.

2) Yamamoto Y., Tsutsumi Y., Yoshioka Y., Nishibata T., Kobayashi K., Okamoto T., Mukai Y., Shimizu T., Nakagawa S., Nagata S. and Mayumi, T. : Site-specific PEGylation of a lysine-deficient TNF-alpha with full bioactivity. Nat. Biotechnol., 21 : 546-552, 2003.

3) Shibata H., Yoshioka Y., Ikemizu S., Kobayashi K., Yamamoto Y., Mukai Y., Okamoto T., Taniai M., Kawamura M., Abe Y., Nakagawa S., Hayakawa T., Nagata S., Yamagata Y., Mayumi T., Kamada H. and Tsutsumi, Y. : Functionalization of tumor necrosis factor-alpha using phage display technique and PEGylation improves its antitumor therapeutic window. Clin. Cancer Res., 10 : 8293-8300, 2004.

4) Walsh G. : Therapeutic insulins and their large-scale manufacture. Appl. Microbiol. Biotechnol., 67 : 151-159, 2005.

5) Dideriksen L. H., Jorgensen L. N. and Drejer, K. : Carcinogenic effect on female rats after 12 months administration of the insulin analogue B10 ASP. Diabetes, 41 : 143A, 1992.

6) Drejer K. : The bioactivity of insulin analogues from *in vitro* receptor binding to *in vivo* glucose uptake. Diabetes Metab. Rev., 8 : 259-285, 1992.

7) Schellekens H. : The immunogenicity of biopharmaceuticals. Neurology, 61 : S11-12, 2003.

8) Schllekens H. and Casadevall N. : Immunogenicity of recombinant human proteins: cause and consequences. J. Neurol., 251 (Suppl 2) : II/4-II/9, 2004.

(堤 康央／石井明子／早川堯夫)

Creation of Novel Cell-Penetrating Peptides for Intracellular Drug Delivery Using Systematic Phage Display Technology Originated from Tat Transduction Domain

Haruhiko KAMADA,*[,a] Takayuki OKAMOTO,[b,c] Maki KAWAMURA,[a,b] Hiroko SHIBATA,[a,b] Yasuhiro ABE,[a,b] Akiko OHKAWA,[a,b] Tetsuya NOMURA,[a,b] Masaki SATO,[a,b] Yohei MUKAI,[a,b] Toshiki SUGITA,[a,b] Sunao IMAI,[a,b] Kazuya NAGANO,[a,b] Yasuo TSUTSUMI,[a,b] Shinsaku NAKAGAWA,[b] Tadanori MAYUMI,[d] and Shin-ichi TSUNODA[a]

[a] *Laboratory of Pharmaceutical Proteomics, National Institute of Biomedical Innovation; 7–6–8 Asagi, Saito, Ibaraki, Osaka 567–0085, Japan:* [b] *Department of Biopharmaceutics, Graduate School of Pharmaceutical Sciences, Osaka University; 1–6 Yamadaoka, Suita, Osaka 565–0871, Japan:* [c] *Department of Molecular Pathobiology, Mie University School of Medicine; 2–174 Edobashi, Tsu, Mie 514–8507, Japan: and* [d] *Department of Cell Therapeutics, Graduate School of Pharmaceutical Sciences, Kobe Gakuin University; 518 Arise, Ikawadani, Nishi-ku, Kobe 651–2180, Japan.*
Received March 14, 2006; accepted November 13, 2006; published online November 16, 2006

Many biologically active proteins need to be delivered intracellularly to exert their therapeutic action inside the cytoplasm. Cell penetrating peptides (CPPs) have been developed to efficiently deliver a wide variety of cargo in a fully biological active form into a range of cell types for the treatment of multiple preclinical disease models. To further develop this methodology, we established a systematic approach to identify novel CPPs using phage display technology. Firstly, we screened a phage peptide library for peptides that bound to the cell membrane. Secondly, to assess functionality as intracellular carriers, we recombined cDNAs of binding peptides with protein synthesis inhibitory factor (PSIF) to create fusion proteins. Randomly chosen clones were cultured and expression of peptide-PSIF fusion proteins induced, followed by screening of protein synthesis activity in cells. Using this systematic approach, novel and effective CPPs were rapidly identified. We suggest that these novel cell-penetrating peptides can utilized as drug delivery tools for protein therapy or an analytical tool to study mechanisms of protein transduction into the cytoplasm.

Key words cell penetrating peptide; phage display; Tat

Many biologically active compounds, including a variety of large molecules, need to be delivered intracellularly to exert their therapeutic action inside the cytoplasm or within the nucleus or other specific organelles. An important requirement in the use of proteins in this context (ex. kinases, phosphatases, transcriptional factors) is the ability of these molecules to efficiently penetrate across the cell membrane. However, the plasma membrane of cells is largely impermeable to proteins and peptides. Recently, it was discovered that certain short peptide sequences, composed mostly of basic, positively charged amino acids (*e.g.* Arg, Lys and His), have the ability not only to transport themselves across cell membranes,[1—3] but also to carry attached molecules (proteins, DNA, or even large metallic beads) into cells.[4—6] These basic sequences are now commonly known as protein transduction domains or cell-penetrating peptides (CPPs) and have been successfully employed to transport cargo proteins across a variety of cell membranes.[7] Cellular delivery using CPPs has several advantages over conventional techniques; indeed, it is efficient across a range of cell types and can be applied to cells *en masse*.[8]

It has been proposed that the Tat transduction domain of HIV is first endocytosed into a caveola compartment and secondarily released into the cytoplasm, following vesicle disruption.[9] Once CPP binds to the cell surface heparan sulfate proteoglycan (HSPG), the CPP-fused protein is internalized *via* a lipid raft-mediated pathway. Additionally, the mechanisms responsible for CPP mediated cargo internalization estimated with regard to enter the cells *via* macropinocytosis[10] and/or through clathrin-mediated endocytosis,[11] or possibly *via* an unknown alternative mechanism. In spite of some common features of these peptides, particularly their highly cationic nature, their structural diversity has fuelled the idea that the penetrating mechanism is not the same for CPPs of different types. As such, the mechanism(s) of internalization of CPPs has not been resolved yet.[7]

Given the potency of the Tat-derived CPPs in mediating the cellular uptake of small and large macromolecular cargos, as demonstrated within the last few years, a large number of laboratories have exploited this system as a tool for transcellular penetration of cultured cells.[12] Most of these applications are based on the fusion of the protein transduction domain of Tat to the protein of interest, either at the N- or C-terminus, followed by addition of the recombinant fusion protein to the culture medium of the cells of interest. It is clear that CPPs are novel vehicles for the rapid translocation of cargo into cells, and exhibit the properties that make them potential drug delivery agents.[13] However, there are problems in respect to a decrease in the rate and efficiency of translocation for large proteins that has not yet been overcome. Accordingly, a large number of different CPPs have been explored to promote translocation of various types of useful cargo, ranging from small molecules to proteins and large supramolecular particles, with great efficiency and reasonable velocity.

We previously showed that the gene III proteins (pIII) of M13 filamentous phage could be used to display mutant protein, with these modified proteins showing fully functional binding to receptor and consequent biological activities.[14,15] Recently, we established a novel whole cell panning method,

* To whom correspondence should be addressed. e-mail: kamada@nibio.go.jp

which selected cell adhesive phage-displayed peptides and, subsequently, a cohort of these peptides having cell penetrating qualities *via* the use of PSIF (protein synthesis inhibitory factor). In this study, we constructed a Tat-based mutant peptide library using this phage display system. Moreover, we demonstrated the direct selection of a unique cell-binding activity utilizing whole cell panning methods and the screening of internalizing peptide using peptide-PSIF fusion protein.

MATERIALS AND METHODS

Cell Line Human epidermoid carcinoma A431 cells were grown in Dulbecco's Modified Eagle's Medium (DMEM) supplemented with 10% fetal calf serum (FCS) in 5.0% CO_2 at 37 °C. Human adenocarcinoma Hela cells were grown in DMEM supplemented with NEAA and 10% FCS. Chinese hamster ovary (CHO)-K1 cells were grown in Ham's F12K medium supplemented with 2 mM L-glutamine and 10% FCS.

Preparation of Phage Peptide Library Primers shown below and used in library construction were purchased from Hokkaido System Science Inc. The phage-display vector pCANTAB-5E was used as a phagemid vector for the generation of the peptide-pIII fusion gene repertoires (Fig. 1). To construct a DNA fragment library encoding 13 amino acid peptides, primers P-oligo1 and P-ologo2 were annealed and elongated with the Klenow fragment in the presence of nucleotide triphosphates. These cDNA-encoding peptide library products were purified with QIAquick® Gel Extraction Kit (QIAGEN) and used as templates for PCR with primers pCANTAB-Hind and Not I Ext to generate the pIII fusion gene repertoires. The peptide-encoding genes were digested with the restriction enzymes HindIII and NotI, agarose gel-purified, and ligated into pCANTAB-5E, which was cut with the same restriction enzyme. The ligated products were electroporated into *E. coli* TG1 cells, plated on modified LB medium (Invitrogen) containing 2% glucose and 50 μg/ml ampicillin, and then incubated overnight at 37 °C. The clones were scraped off the plates into 2YT medium with 10% glycerol and subsequently stored at −70 °C. P-oligo1; 5′-GAT TAC GCC AAG CTT TGG AGC CTT TTT TTT GGA GAT TTT CAA CGT GAA AAA ATT ATT ATT CGC AAT TCC TTT AGT TGT TCC TTT CTA TGC GGC CCA GCC GGC CAT GGC C-3′, P-oligo2; 5′-CGG CGC ACC TGC GGC CGC SNN SNN CGG SNN SNN SNN CTG SNN SNN SNN SNN SNN ACC GGC CAT GGC CGG CTG GGC CGC ATA GAA AGG-3′, pCANTAB-Hind; 5′-GGA AAC AGC TAT GAC CAT GAT TAC GCC AAG-3′, Not I Ext; 5′-GCG GCC TTG TCA TCG TCA TCC TTG TAG TCT GCG GCC GC-3′.

Rescue of Peptide-Phage To rescue the peptide-phage library, 1 l of 2YT medium, containing 2% glucose, and 100 μg/ml of ampicillin, was inoculated from the glycerol stock library. The culture was shaken at 37 °C until OD600 nm=0.4 and 3.2×10^8 plaque forming units of M13KO7 helper phage (Invitrogen) were added. After 30 min incubation at room temperature with shaking, the culture was centrifuged and the pellet recovered. The pellet was then incubated with 50 μg/ml of kanamycin and 100 μg/ml of ampicillin within 2YT medium and grown for 6 h at 37 °C. The phage was purified by standard polyethylene glycol precipitation and filtration with a 0.45 μm PVDF filter (Millipore). Peptide-phage which did not express the objective peptide were removed by a FLAG panning method, as described previously.

Biopanning Method We used a slightly modified procedure from that found in the literature. Briefly, 1.0×10^6 A431 cells were harvested in 6 well culture plates and incubated for 24 h at 37 °C within a 5.0% CO_2 incubator until the logarithmic phase of growth was reached. The culture plates were washed with PBS 3 times and 2% BSA Opti-MEM® (Invitrogen) added 2 h prior to the addition of the peptide-phage. Cells were incubated with the peptide-phage library for 2 h at 37 °C with shaking every 15 min during the round of panning. Following this, the cells were washed twenty times with PBS at room temperature. After washing, the cells were lysed with 1 ml of 100 mM HCl and neutralized with 0.5 ml of 1 M Tris–HCl, pH 8.0. One-hundred microliters lysate was used

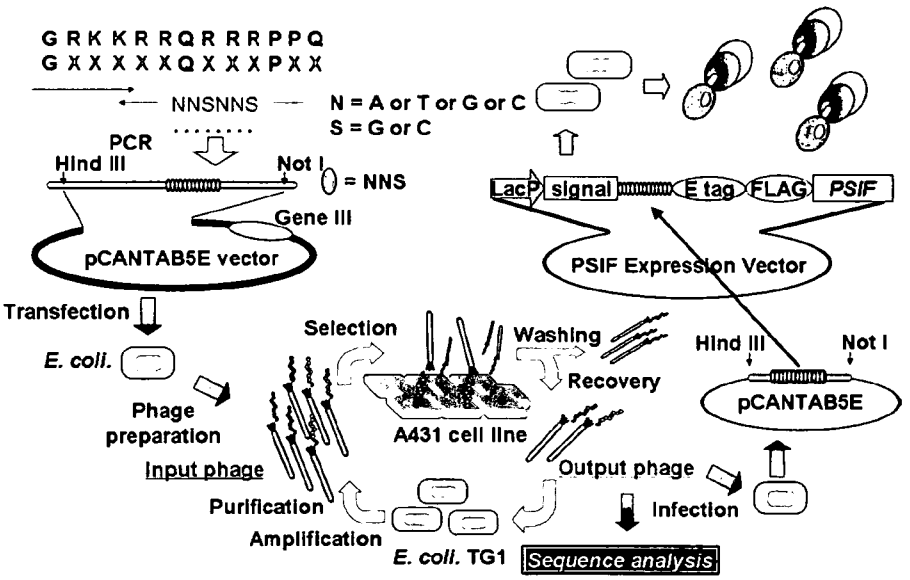

Fig. 1. Schema for Screening CPPs

to infect 0.3 ml of *E. coli* TG1 cells, with phage being rescued as described above and used in the next round of selection.

Expression and Purification of a Peptide-PSIF Fusion Protein Protein synthesis inhibitory factor (PSIF, PE fragment) is an approximately 40 kD fragment of the bacterial exotoxin (GenBank Accession No. K01397) derived from *Pseudomonas aeruginosa* (ATCC strain No. 29260). PSIF lacks its cell binding domain, and is the truncated form of *Pseudomonas aeruginosa* exotoxin, which is a non-toxic protein outside of the cell. One (Dr. Tsunoda) of us cloned the cDNA for PSIF from *Pseudomonas aeruginosa*, Migula by PCR using the primer set 5′-GAT GAT CGA TCg cgg ccg caG GTG CGC CGG TGC CGT ATC CGG ATC CGC TGG AAC CGC GTG CCG CAg act aca aag acg acg acg aca aaC CCG AGG GCG GCA GCC TGG CCG CGC TGA CC-3′ and 5′-GAT CGA TCG ATC act agt CTA cag ttc gtc ttt CTT CAG GTC CTC GCG CGG CGG TTT GCC GGG-3′. The fusion protein, denoted peptide-PSIF, consisted of peptide at the N-terminus and a PSIF at the C-terminus. First, the peptide gene containing phagemid vectors were recovered with QIAprep® Miniprep Kit (QIAGEN) and digested with HindIII and NotI. The peptide gene fragments were then subcloned into PSIF Expression Vector, which is modified from pCANTAB-5E. The fusion proteins were expressed and collected within the supernatant from *E. coli* TG1 cells, with the supernatant being used for cell viability assays.

Cell Viability A431 cells (2.0×10^4) were incubated with 35 μl Opti-MEM® and 10 μl cycloheximide (100 μg/ml) in 96 well plates. Cells were treated with 5 μl peptide-containing supernatant for 24 h and the cell viability was monitored by MTT assay. Twenty-four hours after addition of the peptides, 10 μl of 5 mg/ml MTT (Dojindo) were added to each well and the cells were further incubated at 37 °C for 4 h. Subsequently, the insoluble formazan crystals were solubilized in a solution of 20% SDS containing 0.01 N HCl. Absorbance measurements were taken at λ=595 nm with background subtracted at λ=655 nm. Each sample point was performed in duplicate.

FACS Analysis The specific cell binding activities of peptides towards A431, Hela, CHO-K1 cells were measured by FACScan (Becton Dickinson). Cells were grown in tissue culture flasks to late logarithmic phase. Culture medium was renewed 2 h prior to the addition of the peptide-phage. FITC-labeled peptides were purchased from Genenet Co., Ltd. and 1×10^5 cells were incubated with FITC-labeled peptide for 3 h at 37 °C. For the endocytosis inhibitor assays, FACS analysis was performed after pre-treating A431 cell monolayers at 37 °C with 10 mM methyl-β-cyclodextrin (MβCD; caveola-mediated endocytosis inhibitor) or amiloride (macropinocytosis inhibitor) in serum-free Minimal Essential Medium (MEM) for 30 min, followed by a 1-h co-incubation with FITC labeled-peptide. After three washes with PBS, 0.25% trypsin solution (Gibco BRL) was added and incubated for 15 min to digest non-specific binding peptides. After three additional washes, cells were resuspended in PBS/4% paraformaldehyde and analyzed using FACScan.

RESULTS

Construction of Phage Peptide Library and Quality Check The pCANTAB-5E phagemid library used here has previously been screened successfully for mutant protein which binds to receptors.[14,15] Additionally, we previously reported the identification and characterization of a series of cationic peptides, similar to the CPP derived from Tat, which are able to penetrate large protein complexes into a wide variety of cells, including fibroblasts. Here, we made a novel phage peptide library, which altered ten amino acids within the Tat transduction domain (13 amino acids). The library of the TAT-based CPPs was made *via* the annealing and elongation of two mutated primers, followed by PCR amplification and cloning into a phage expression system The peptide-encoding cDNA library was placed into a phagemid vector and expressed as a fusion protein with phage coat protein, pIII. We confirmed the identity and sequence distribution of this phage peptide library by DNA sequencing (Table 1). In this context, eight clones which were sequenced showed independent sequences, highlighting the distribution of this phage peptide library.

Concentration of Binding Peptides with a Cell Panning Method The constructed peptide phage library was selected *in vitro* against A431 cells. Selection was performed as described in the Materials and Methods section, with a view to enriching for peptides displaying cell binding activity. With respect to the phage panning and amplification processes, which were repeated for one to four rounds, the output/input ratio was found to increase in a manner dependent on cycle number (Fig. 2). These results indicated that the peptides having an affinity for A431 cells were enriched gradually by this cell panning approach.

Identification of A431 Cell Binding Peptides Peptide clones that became internalized in A431 cells were isolated by four rounds of selection. In order to select only internalized phage-derived peptides, cells were incubated with super-

Table 1. Random TAT Peptide Library Sequence before Panning

Clone	Sequence
1	GMHINGQSNPPHA
2	GGMHESQSHMPGD
3	GTQAFLQQFEPWI
4	GIKHSPQQISPRW
5	GILCIQQDHQPLG
6	GFKLSSQAVAPLQ
7	GSIRAPQGDSPWP
8	GTRHGIQTQPPNN

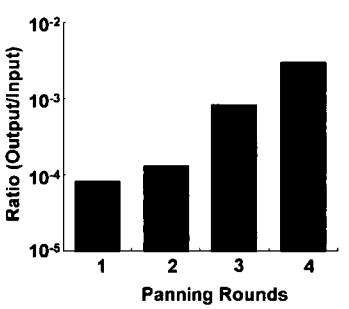

Fig. 2. Enrichment of Phage Clones by Biopanning

A431 cells were incubated with 4×10^{10} titer phage. After washing with PBS, binding phages were recovered and the titer was determined. The index of enrichment was evaluated with input/output ratio.

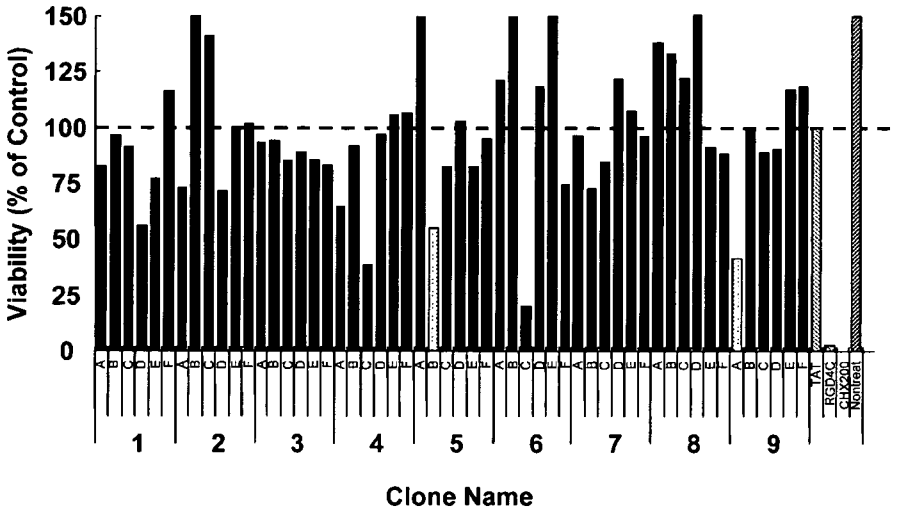

Fig. 3. Measurement of Penetrating Activity as an Index of Cytotoxicity to A431 Cells

PSIF-CPP fusion genes were transformed into TG1 cells, with resulting fusion proteins then recovered from the supernatant. The cytotoxicity of the supernatant was then assessed to examine the activity of the CPPs. Cell viability in response to fusion proteins was compared with that exhibited by exposure to the parent Tat13 peptide (cell viability=100%), and by exposure to 200 μg/ml cycloheximide (CHX; cell viability=0%).

natant collected from *E. coli* cells. After four rounds of selection, an enrichment in the order of 10^5 was obtained. The random insert region of the single-stranded DNA from individual clones, following the fourth round of selection, was sequenced and the amino acid coding sequence deduced. To identify peptides capable of facilitating internalization, we developed a screening method using an M13 peptide phage display library. We incubated 1×10^6 A431 cells, with 4×10^{10} phage from a 13-mer peptide M13 phage display library for 2 h at 37 °C. Following four rounds of screening, we isolated phage from 28 plaques and determined the identity of the encoded peptides by DNA sequencing (Table 2). Twenty-eight of the peptide sequences were found in at least 15 independent plaques and were selected for further analysis.

Evaluation of Cell Penetrating Activity of CPPs Following creation of the peptide library (input phage library), we expressed these Tat-based CPPs as fusion proteins with PSIF. From this, 54 candidates were found that exhibited lower cytotoxic activity than the parent Tat peptide (data not shown). These results indicated that the penetrating activity is remarkably decreased as a consequence of random conversion of amino acids within the Tat transduction domain. In addition, we made the PSIF-fused peptide library after fourth round panning (Fig. 3). In screening this peptide library, a tryptophan-rich (GSSSWWQRWWPPW) peptide was identified (Table 2). However, this peptide did not exhibit cytotoxicity when recombined with PSIF. This result indicated that this tryptophan-rich peptide binds to the cell membrane but does not penetrate through to the cytoplasm. Next, we reconfirmed that fixation of the cells significantly affected the cellular distribution of peptides (Fig. 4). 435B peptide (GPFHFYQFLFPPV) and 439A peptide (GSPWGLQHHPPRT) showed internalization characteristics similar to those of the parent Tat peptide. These FITC-labeled peptides did not show cytotoxicity at a dose of 10 μM. However, the two another clone (434C and 436C peptide) does not TAT-derived peptide , which is not consist of 13 amino acid or occur the flameshift, respectively. So we were excluded these two clones from followed experiment.

Table 2. Random Tat Peptide Library Sequence after 4th Panning

Clone	Sequence
1	GPMESLQAFWPPW
2	GSSSWWQRWWPPW
3	GSSSWWQRWWPPW
4	GVFLLKQVPQPSH
5	GSSSWWQRWWPPW
6	GRLWWLQLFEPGH
7	GLRKVPQSVPPDM
8	GSSSWWQRWWPPW
9	GHFLKPQVLRPTR
10	GQFMMRQYWPPVH
11	GSSSWWQRWWPPW
12	GSSSWWQRWWPPW
13	GSSSWWQRWWPPW
14	GLLKYQQWASPLC
15	GYFWYDQPWQPEQ
16	GRNHYIQRDNPVS
17	GVFHVLQNAIPQY
18	GSSSWWQRWWPPW
19	GTMPNMQHHDPAR
20	GSSSWWQRWWPPW
21	GSSSWWQRWWPPW
22	GSSSWWQRWWPPW
23	GTRYLVQYLFPHL
24	GRPATQQGLTPAR
25	GYIGTYQQWNPPP
26	GSSSWWQRWWPPW
27	GSSSWWQRWWPPW
28	GSSSWWQRWWPPW

Uptake of FITC-Labeled Peptides into Human and Murine Cells To address the question of whether 435B and 439A peptides were more active than the parent Tat peptide, peptides conjugated to FITC were constructed. Cellular uptake of both peptides were judged by flow cytometric analysis on human carcinoma A431 and Hela and CHO cells. Assuming that the surface-adsorbed 435B and 439A peptides were susceptible to tryptic degradation, we washed the cells five times with PBS and treated them with trypsin prior to assessing the amount of the internalized peptide. On A431

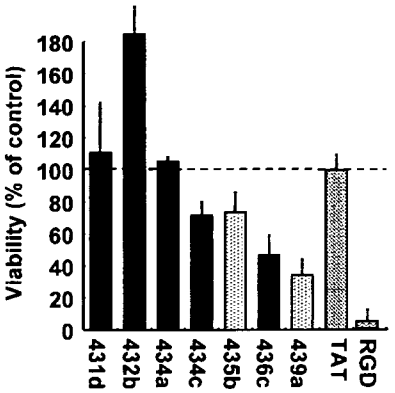

Fig. 4. Evaluation of Cell Penetrating Activity of Individual Clones

Cell penetrating activity was reconfirmed using the same method as that referred to in Fig. 3. Cell viability in response to fusion proteins was compared with that exhibited by exposure to the parent Tat13 peptide (cell viability=100%), and by exposure to 200 μg/ml cycloheximide (CHX; cell viability=0%).

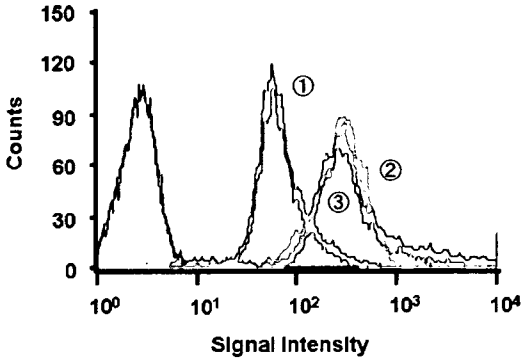

Fig. 5. Intracellular Penetrating Activity of FITC-Labeled CPPs on A431 Cells

Ten micromolar FITC-labeled 439A peptide (①), 435B peptide (②) and parent Tat peptide (③) were added to A431 cells. Gray area showed the distribution of non-treated cells. Following trypsinization, the quantity of penetrating peptide was evaluated in cells according the level of fluorescence intensity.

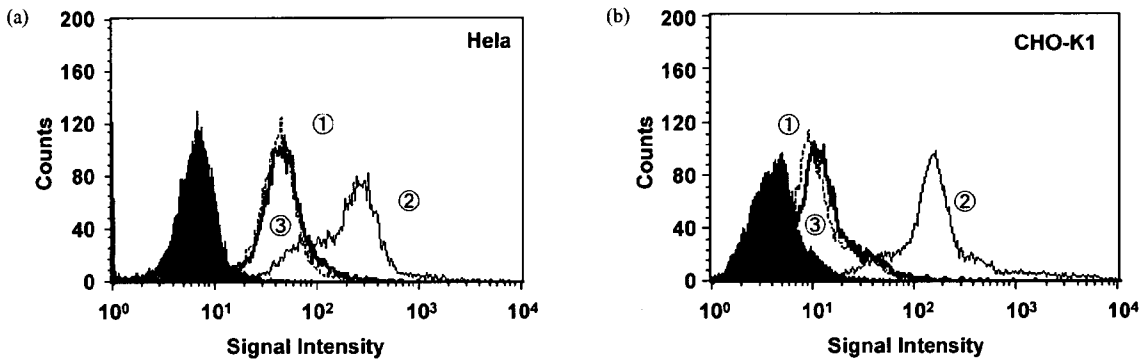

Fig. 6. Intracellular Penetrating Activity of FITC-Labeled CPPs on Human and Murine Cell Lines

Ten micromolar FITC-labeled 439A peptide (①), 435B peptide (②) and parent Tat peptide (③) were added to Hela (a) and CHO (b) cells. Gray area showed the distribution of non-treated cells. Following trypsinization, the quantity of penetrating peptide was evaluated in cells according the level of fluorescence intensity.

cells, the efficiency in terms of cell penetration between the parent Tat peptide and 435B peptide was almost the same, though the penetrating activity of the 439A peptide was decreased about 10 fold compared to the parent Tat peptide and 435B peptide (Fig. 5). However, on Hela and CHO cells, the efficiency of cell penetration between the parent Tat peptide and 439A peptide was almost the same, though the penetrating activity of the 435B peptide was increased about 10 fold compared to the parent Tat peptide and 439A peptide (Figs. 6a, b).

Inhibition of Endocytic Internalization Several studies were done to investigate the involvement of macropinocytosis or caveolae/raft-dependent endocytosis on peptide transduction domain such as TAT. The effect of the specific macropinocytosis inhibitor, amiloride, on TAT peptide penetration was determined. As seen in Fig. 7, treatment with amiloride did not inhibit 435B and 439A pepetration. Additionally, Methyl-β-cyclodextrin (MβCD)-sensitive caveolae/raft-dependent endocytosis of 435B and 439A peptides was detected, internalization of 435B and 439A *via* transduction is significantly affected by MβCD treatment.

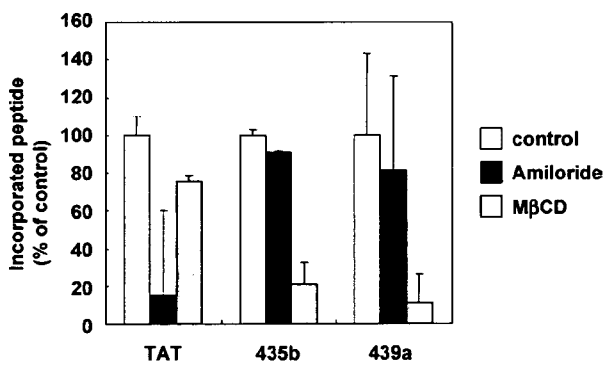

Fig. 7. Inhibitory Effects of Amiloride and MβCD for Peptide Incorporation on A431 Cells

FITC-labeled 435B peptide and 439A peptide were added to cells after amiloride and MβCD pre-incubated. The quantity of penetrating peptide was evaluated by FACS analysis according the mean of fluorescence intensity.

DISCUSSION

In an effort to search for novel CPPs, we have screened an M13 peptide phage display library comprised of CPPs based on the Tat transduction domain. From this screening approach, we have identified peptides that displayed a capability for cell penetration. In particular, a screen using A431 cells resulted in identification of peptide 435B and 439A that is able to penetrate cultured cells *in vitro* efficiently. Thus, this method of screening for CPPs using phage peptide li-

braries can be readily applied to select from a wide variety of possible peptides.

Whether the parent Tat peptide shows the penetrating capability of other known CPPs is uncertain.[12,16] The RGD peptide has long been used to facilitate the transport of bioactive molecules through adsorptive endocytosis.[17] However, comparison of short oligolysine peptides to that of equivalent length polymers of arginine showed that oligoarginine was much more efficient in carrying GFP into cultured cells.[18] Conversely, the ability of short oligolysine peptides, from 6 to 12 residues in length, has been shown to be more efficient than oligoarginine in carrying larger macromolecules (60—500 kDa) into cultured cells. In this study, the 435B and 439A peptides contained hardly any basic amino acids but still displayed an ability to mediate cell penetration more efficiently than the parent Tat peptide. This result indicated that the cell penetrating activity of CPPs is controlled not only by the electrical charge but also by the structural characteristics. Practically, it is known that the amino acid component and associated tertiary structure of peptides are essential for cell penetrating activity.[19] We did not examine our peptides on a structural level; however, the results presented here suggest the importance of hydrophobicity, as hydrophobic amino acids were enriched by sequential biopanning.

It has been theorized that the ionic interaction between positively charged Arg residues in these CPPs and the negatively charged phosphate head group of the membrane lipid bilayer plays a key role in CPP membrane interaction.[20] However, the exact mechanism by which these CPPs operate is still largely unknown. Work performed by several investigators has shown that Tat binds heparin and that this heparin/Tat interaction involves the basic domain of Tat.[21] Meanwhile, previous study showed that the histidine residues of peptide sequence might enhance an endosomal escape of the cargo.[22] In this study, the 435A and 439B peptides did not show enrichment of basic amino acids, but did exhibit an increase in proportion of hydrophobic amino acids. Several numbers of histidine residues were included in 435B and 439A peptide sequence compared to native TAT peptide. Accordingly, it is possible that these peptides do not penetrate through the binding of cell surface receptors such as HSPG but escape from endosome efficiently. Whereas the conformation of these peptides should be examined, our results suggest that the 435B and 439A peptides penetrate the cell membrane independently of cell surface receptor.

In this study, the transduction efficiency was observed to be different between the peptides fused with PSIF and those labeled with FITC. We think there are two ideas to explain this discrepancy. Firstly, the molecular size and structure of the respective cargo is different. Secondly, there is some possibility that the intracellular kinetics is different between the parent Tat peptide and our peptides. It is thought that the parent Tat peptide is transferred to nuclei after penetrating the cell membrane, while our mutant peptide-PSIF conjugate diffuses throughout the cytoplasm. We are currently examining the intracellular kinetics of these peptides in an effort to resolve this issue.

In this study, our peptides have a unique sequence compared to preexisting CPPs. These peptides are able to introduce a large molecule into the intracellular space more efficiently than the parent Tat peptide, the latter which is known to have a high level of transduction ability. Using these peptides, efficient introduction of large molecules to the cytoplasm is accomplished. As such, one could readily conceive of using these peptides to target disease-related proteins, revealed from extensive-omic analysis. Furthermore, our peptides can be used as analytical tools to explore the mechanism(s) of peptide penetration.

Acknowledgements This study was supported by the following grants: a Grant-in-Aid for Scientific Research (No. 17689008, 17016084, 17790135, 16790534, 18015055, 18659047) from the Ministry of Education, Culture, Sports, Science and Technology of Japan; a Grant-in-Aid for Scientific Research from the Japan Society for the Promotion of Science; Health and Labour Sciences Research Grants from the Ministry of Health, Labour; a Research Grant from the New Energy and Industrial Technology Development Organization (NEDO; No. 03A47016a), and JSPS Research Fellowships for Young Scientists (No. 08476, 08841, 09131) from the Japan Society for the Promotion of Science.

REFERENCES

1) Frankel A. D., Pabo C. O., *Cell*, **55**, 1189—1193 (1988).
2) Derossi D., Joliot A. H., Chassaing G., Prochiantz A., *J. Biol. Chem.*, **269**, 10444—10450 (1994).
3) Futaki S., Suzuki T., Ohashi W., Yagami T., Tanaka S., Ueda K., Sugiura Y., *J. Biol. Chem.*, **276**, 5836—5840 (2001).
4) Lewin M., Carlesso N., Tung C. H., Tang X. W., Cory D., Scadden D. T., Weissleder R., *Nat. Biotechnol.*, **18**, 410—414 (2000).
5) Ryu J., Lee H. J., Kim K. A., Lee J. Y., Lee K. S., Park J., Choi S. Y., *Mol. Cells*, **17**, 353—359 (2004).
6) Schwarze S. R., Ho A., Vocero-Akbani A., Dowdy S. F., *Science*, **285**, 1569—1572 (1999).
7) Zorko M., Langel U., *Adv. Drug Deliv. Rev.*, **57**, 529—545 (2005).
8) Wadia J. S., Dowdy S. F., *Adv. Drug Deliv. Rev.*, **57**, 579—596 (2005).
9) Ferrari A., Pellegrini V., Arcangeli C., Fittipaldi A., Giacca M., Beltram F., *Mol. Ther.*, **8**, 284—294 (2003).
10) Wadia J. S., Stan R. V., Dowdy S. F., *Nat. Med.*, **10**, 310—315 (2004).
11) Richard J. P., Melikov K., Brooks H., Prevot P., Lebleu B., Chernomordik L. V., *J. Biol. Chem.*, **280**, 15300—15306 (2005).
12) Brooks H., Lebleu B., Vives E., *Adv. Drug Deliv. Rev.*, **57**, 559—577 (2005).
13) Lindgren M., Hallbrink M., Prochiantz A., Langel U., *Trends Pharmacol. Sci.*, **21**, 99—103 (2000).
14) Yamamoto Y., Tsutsumi Y., Yoshioka Y., Nishibata T., Kobayashi K., Okamoto T., Mukai Y., Shimizu T., Nakagawa S., Nagata S., Mayumi T., *Nat. Biotechnol.*, **21**, 546—552 (2003).
15) Shibata H., Yoshioka Y., Ikemizu S., Kobayashi K., Yamamoto Y., Mukai Y., Okamoto T., Taniai M., Kawamura M., Abe Y., Nakagawa S., Hayakawa T., Nagata S., Yamagata Y., Mayumi T., Kamada H., Tsutsumi Y., *Clin. Cancer Res.*, **10**, 8293—8300 (2004).
16) Futaki S., *Int. J. Pharm.*, **245**, 1—7 (2002).
17) Gresham H. D., Goodwin J. L., Allen P. M., Anderson D. C., Brown E. J., *J. Cell Biol.*, **108**, 1935—1943 (1989).
18) Han K., Jeon M. J., Kim S. H., Ki D., Bahn J. H., Lee K. S., Park J., Choi S. Y., *Mol. Cells*, **12**, 267—271 (2001).
19) Lindberg M., Jarvet J., Langel U., Graslund A., *Biochemistry*, **40**, 3141—3149 (2001).
20) Ziegler A., Blatter X. L., Seelig A., Seelig J., *Biochemistry*, **42**, 9185—9194 (2003).
21) Rusnati M., Tulipano G., Urbinati C., Tanghetti E., Giuliani R., Giacca M., Ciomei M., Corallini A., Presta M., *J. Biol. Chem.*, **273**, 16027—16037 (1998).
22) Midoux P., Monsigny M., *Bioconjug. Chem.*, **10**, 406—411 (1999).

Available online at www.sciencedirect.com
ScienceDirect
Biochimica et Biophysica Acta 1774 (2007) 1029–1035
Biochimica et Biophysica Acta
BBA
www.elsevier.com/locate/bbapap

Role of amino acid residue 90 in bioactivity and receptor binding capacity of tumor necrosis factor mutants

Hiroko Shibata [a,b], Haruhiko Kamada [a,c,*], Kyoko Kobayashi-Nishibata [b], Yasuo Yoshioka [c], Toshihide Nishibata [b], Yasuhiro Abe [a,b], Tetsuya Nomura [a,b], Hiromi Nabeshi [a], Kyoko Minowa [a], Yohei Mukai [a,b], Shinsaku Nakagawa [b], Tadanori Mayumi [d], Shin-ichi Tsunoda [a,c], Yasuo Tsutsumi [a,b,c]

[a] *National Institute of Biomedical Innovation, 7-6-8 Saito-Asagi, Ibaraki, Osaka 567-0085, Japan*
[b] *Department of Biotechnology and Therapeutics, Graduate School of Pharmaceutical Sciences, Osaka University, 1-6 Yamadaoka, Suita, Osaka 565-0871, Japan*
[c] *The Center for Advanced Medical Engineering and Informatics, Osaka University, 1-6 Yamadaoka, Suita, Osaka 565-0871, Japan*
[d] *Faculty of Pharmaceutical Sciences, Kobe-gakuin University, 518 Arise, Igawadani, Nishi-ku, Kobe 651-2180, Japan*

Received 12 March 2007; received in revised form 3 May 2007; accepted 3 May 2007
Available online 22 May 2007

Abstract

We have previously produced two bioactive lysine-deficient mutants of TNF-α (mutTNF-K90R,-K90P) and found that these mutants have bioactivity superior to wild-type TNF (wtTNF). Because these mutants contained same amino acid except for amino acid 90, it is unclear which amino acid residue is optimal for showing bioactivity. We speculated that this amino acid position was exchangeable, and this amino acid substitution enabled the creation of lysine-deficient mutants with enhanced bioactivity. Therefore, we produced mutTNF-K90R variants (mutTNF-R90X), in which R90 was replaced with other amino acids, to assay their bioactivities and investigated the importance of amino acid position 90. As a result, mutTNF-R90X that replaced R90 with lysine, arginine and proline were bioactive, while other mutants were not bioactive. Moreover, these three mutants showed bioactivity as good as or better than wtTNF. R90 replaced with lysine or arginine had especially superior binding affinities. These results suggest that the amino acid position 90 in TNF-α is important for TNF-α bioactivity and could be altered to improve its bioactivity to generate a "super-agonist".

Keywords: TNF; Mutant; Phage display; Lysine residue; TNF receptors; Structure

1. Introduction

TNF-α is an inflammatory cytokine able to mediate tumor regression in experimental and clinical cancers [1–3]. Attempts to use TNF-α for its cytotoxic property led to the development of several strategies that, in some cases, resulted in the use of TNF-α in clinical trials of tumor immuno-chemotherapy [4–6]. However, a frequent administration at high dose of TNF-α was required to obtain anti-tumor effect because of its poor stability and short half-lives, and resulted in severe side-effects [7]. Therefore, clinical application of TNF-α is still limited. More recently, some groups have reported positive results using melphalan in combination with TNF-α for patients with melanoma [8, 9]. These findings suggest that the enhanced anti-tumor effect of melphalan observed after the combination with TNF-α resulted from potentiation of the TNF-induced accumulation of melphalan into tumor accompanied by increased tumor vascular permeability [10]. The improved retention of TNF-α in the vascular space and the resultant decrease in transfer of TNF-α to normal tissues is expected to reduce the side effects of TNF-α therapy [11]. Thus, improving the circulation time of TNF-α may not only enhance its anti-tumor effects but also vascular permeability activity without increasing its side effects, resulting in longer bioavailability.

One of the most useful ways of enhancing the plasma half-lives of proteins is to conjugate them with polyethylene glycol (PEG) or other water-soluble polymeric modifiers [12–14]. The

* Corresponding author. National Institute of Biomedical Innovation, 7-6-8 Saito-Asagi, Ibaraki, Osaka 567-0085, Japan.
E-mail address: kamada@nibio.go.jp (H. Kamada).

1570-9639/$ - see front matter © 2007 Elsevier B.V. All rights reserved.
doi:10.1016/j.bbapap.2007.05.003

covalent conjugation of proteins with PEG (PEGylation) increases their molecular size and steric hindrance, both of which depend on the properties of the PEG attached to the protein. This prevents renal excretion and improves their proteolytic stability while decreasing their immunogenicity and hepatic uptake. We have also reported that optimal PEGylation of bioactive proteins could selectively improve their in vivo therapeutic potency and reduce side-effects [15, 16]. However, the PEGylation of proteins was mostly nonspecific and targeted lysine residues, some of which were in or near an active site. As a result, the PEGylation of proteins was accompanied by a significant loss of their specific activities in vitro [14, 17]. Thus, the clinical application of PEGylated proteins has been limited. To overcome the problems of PEGylation, we attempted to develop a novel strategy for site-specific mono-PEGylation of TNF-α to improve its antitumor potency in vivo [18, 19]. We produced bioactive lysine-deficient mutants of TNF-α (mutTNFs) from phage libraries expressing mutTNFs in which all of the six lysine residues were replaced with other amino acids. Among these mutant proteins, mutTNF-K90R and mutTNF-K90P have superior bioactivity, especially mutTNF-K90R, which has a 60-fold broader anti-tumor therapeutic window than wild-type TNF-α (wtTNF) [18].

Interestingly, these two mutTNFs were identical except for single amino acid changes at amino acid 90. Other lysine residues (amino acid 11, 65, 98, 112, 124) were replaced with alanine, serine, alanine, leucine, threonine respectively. Our previous study discussed the significance of R90 and P90 in the context of the TNF–TNF receptor structure. In the wtTNF structure, K90 forms a hydrogen bond with E135. This interaction likely stabilizes the loop structure containing residues 84 to 89, which is involved in receptor binding according to the model. In the mutTNF-K90R, arginine also is likely to be involved in hydrogen bonding with E135. The interaction may contribute to the stabilization of the loop structure. To confirm this speculation and clarify the importance of amino acid 90, it is necessary to create mutTNF-K90R variants (mutTNF-R90X) by replacing R90 with other amino acid in mutTNF-K90R, and validate their bioactivity, ability to form trimers, and binding affinity toward receptors. Moreover, the fact that only amino acid 90 substitutions were obtained highlights the importance of amino acid 90 as a key determinant between TNF-α and TNF receptor affinity and for its resulting level of bioactivity. This idea raises the possibility that mutTNFs with stronger bioactivity than mutTNF-K90R are created by the substitution of amino acid 90. Therefore, in this study, we evaluated the binding ability and bioactivity of mutTNF-R90X in order to examine the structural importance of the amino acid position 90 and to obtain mutTNFs with stronger bioactivity.

2. Materials and methods

2.1. Random amino-acid substitution of R90 in mutTNF-R90

The *Escherichia coli* library expressing mutTNF-R90 variants (mutTNF-R90Xs) in which R90 is replaced with other amino acids was constructed by the method as shown in Fig. 1. These mutTNF-R90Xs were also lysine-deficient except when X is lysine. pY02-mutTNF-R90 was used as a PCR template, and the arginine codon of mutTNF-R90 was replaced with the randomized sequence 'NNS (where N and S represent G/A/T/C or G/C, respectively) ' by two-step PCR using 4 primers. Oligo-1: 5′-cgG GCC AAG GCT GCC CCT CCA CCC ATG TGC TCC TCA CCC ACA CCA TCA GCC GCA TCG CCG TCT CCT ACC AGA CCN NS GTC AAC CTC CTC TCT GCC ATC-3′, Oligo-2 : 5′-GCC CAG ACT CGG CAA AGT CGA GAT AGT CGG GCC GAT TGA TCT CAG CGC T-3′, Oligo-3 : 5′-TGT ACC TTA TCT ACT CCC AGG TCC TCT TCT CGG GCC AAG GCT GCC CCT C-3′, Oligo-4 : 5′-GCC CAG ACT CGG CAA AGT CGA GAT AGT CGG GCC GAT TGA TCT CAG CGC T-3′. First PCR was carried out using Oligo-1 and -2. The PCR condition was cycled 30 times at 95 °C for 60 s, 57 °C for 60 s, and 68 °C for 60 s. PCR products (251 bp) were purified with QIAquick PCR purification Kits (QIAGEN, Valencia) and used as templates for second PCR. The second PCR was carried out using Oligo-

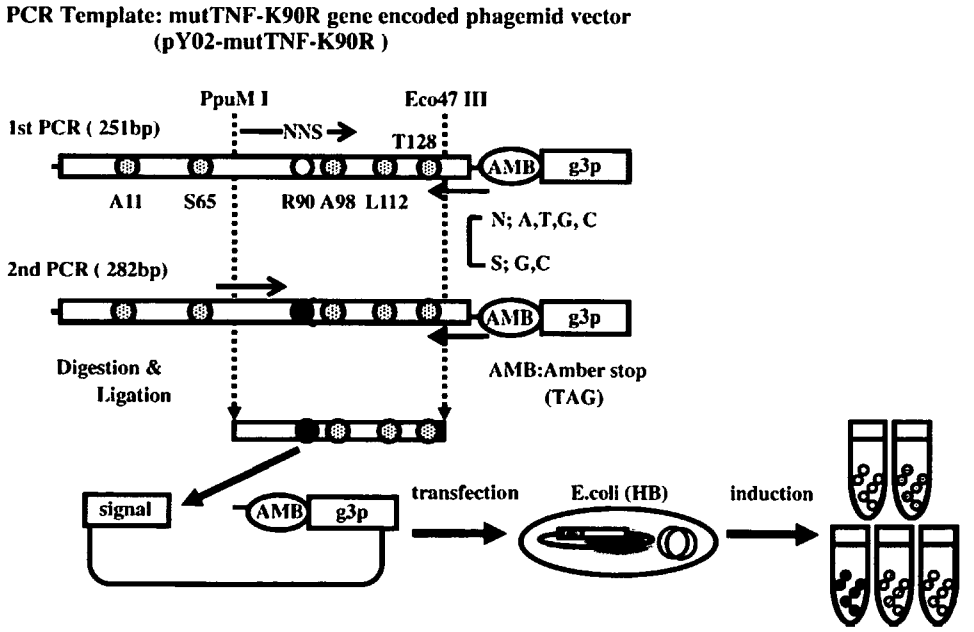

Fig. 1. Construction of mutTNF-R90X *E. coli* library.

3 and -4 under the same cycling conditions. Purified PCR products (283 bp) and pY02-mutTNF-K90R were digested with PpuM I and Eco47III. The resulting PCR products were inserted into pY02-mutTNF-K90R using T4 ligase (Roche Diagnostics, IN) at 16 °C for 16 h. Ligated DNAs were purified and introduced into *E. coli* HB2151 using a Bio-Rad Gene Pulser (Bio-Rad Laboratories, CA). The *E. coli* was then grown by culturing at 37 °C in LB agar medium with ampicillin (100 μg/mL) and glucose (2% w/v).

2.2. Preparation of E. coli culture supernatant

Colonies on LB agar medium were picked and grown by culturing at 37 °C in 2-YT medium with ampicillin (100 μg/mL) and glucose (2% w/v) until the OD_{600} of the culture medium reached 0.4. After centrifugation, supernatants were removed, and fresh 2-YT media with ampicillin (100 μg/mL) was added to *E. coli* pellets. After incubation for 6 h supernatants were collected and used for ELISA and bioassay.

2.3. TNF-α ELISA

Human TNF neutralizing monoclonal antibody (4 μg/mL, R&D systems, US) was coated onto Maxisorb immunoplates (NUNC, Denmark). After blocking, *E. coli* supernatant was then added into the plates and incubated at 37 °C for 2 h. The plates were washed three times with PBS and 0.05% Tween PBS and incubated with 200 ng/mL biotinylated anti-human TNF polyclonal antibody (R&D systems, US) at 37 °C for 1 h. After incubation, the plates were washed three times, and incubated with diluted avidin-HRP (Zymed Laboratories, Inc, US) at 37 °C for 1 h. After washing, TMB peroxidase substrate (MOSS, Inc. US) was added, and the absorbance was read at 450 nm / 650 nm using a micro plate reader.

2.4. Cytotoxicity assay

L-M cells, a cell line derived from L929 cells, were maintained in Eagle's Minimum Essential Medium (MEM, Sigma-Aldrich, Inc. Japan) with 1% bovine fetal serum and antibiotics. L-M cells treated with 1 μg/mL actinomycin D were seeded at 3×10^4 cells/well in 96 well plates, and cultured in the presence of *E. coli* supernatants or serially diluted TNFs. After incubation for 24 h, L-M cells were fixed by 25% glutaraldehyde and stained with 0.05% methylene blue for 15 min. After washing, 0.33 N HCl (100 μl) was added to each well, and the absorbance of released dye was measured at 655 nm /415 nm. Recombinant human TNF (R&D systems, US) was used as a standard.

In the case of HEp-2 cells, cells were maintained in RPMI 1640 medium (Sigma-Aldrich, Inc. Japan) with 10% bovine fetal serum, sodium pyruvate (1 mM), 2-mercaptoethanol (50 μM), and antibiotics. Cells were treated with 100 μg/mL cycloheximide, seeded at 4×10^4 cells/well, fixed after 18 h incubation, and used as described above.

2.5. Purification of recombinant proteins

Purification of recombinant proteins was described previously. Briefly, TNFs were produced in *E. coli* BL21(DE3). TNFs were recovered from inclusion bodies, which were washed in Triton X-100 and solubilized in 6 M guanidine–HCl, 0.1 M Tris–HCl, pH 8.0, and 2 mM EDTA. Solubilized protein (10 mg/mL) was reduced with 10 mg/mL dithioerythritol for 4 h at RT and refolded by 100-fold dilution in a refolding buffer, 100 mM Tris–HCl, 2 mM EDTA, 1 M arginine, and oxidized glutathione (551 mg/L). After dialysis with 20 mM Tris–HCl, pH 7.4, containing 100 mM urea, active trimeric proteins were purified by Q-Sepharose and MonoQ chromatography. Additionally, size-exclusion chromatography (Superose 12, GE Healthcare, England) was performed.

2.6. Surface plasmon resonance assay (BIAcore assay)

Human TNFR1 or TNFR2 Fc chimera (R&D systems, US) was diluted to 50 μg/mL in 10 mM sodium acetate buffer (pH 4.5) and immobilized to a CM3 sensor chip using an amine coupling kit (BIAcore, Sweden), which resulted in an increase of 4000–6000 resonance units (RU). During the association phase, mutTNFs or wtTNF diluted in running buffer (HBS-EP) at 26.1 nM, 8.7 nM or 2.9 nM were individually passed over the immobilized TNFRs at a flow rate of 20 μl/min. During the dissociation phase, HBS-EP buffer was applied to the sensor chip at a flow rate of 20 μl/min. Elution was carried out using 20 μl of 10 mM glycine–HCl. The data were analyzed globally with BIA EVALUATION 3.0 software (BIAcore®, Sweden) using a 1:1 binding model.

2.7. Induction of GM-CSF in PC60-hTNFR2 cells

PC60-hTNFR2, which is a cell line transfected with the human TNFR2, was kindly provided by Dr. Vandenabeele, and induction experiments were performed as previously described. PC60-hTNFR2 cells were cultured in RPMI-1640 supplemented with 10% bovine fetal serum, sodium pyruvate (1 mM), 2-ME (50 μM), and puromycin (3 μg/mL). Cells were seeded at 5×10^4 cells/well in 96 well plates with 2 ng/mL IL-1β (Peprotech, US) and serially diluted mutTNFs and wtTNF. After 24 h incubation, production of rat GM-CSF was quantified by ELISA according to the manufacturer's protocol (R&D systems, US).

3. Results

3.1. Phage library construction and bioactivity of mutTNF-R90X in culture supernatant of E. coli

In the first PCR step, DNA fragments (251 bp) in which the codon of R90 was replaced with an NNS sequence were synthesized. In the second PCR step, the first PCR product was extended to the PpuM I site. This second PCR product was digested with PpuM I and Eco47 III, and ligated with the phagemid vector pY02 to express mutTNF-R90X in culture supernatant of *E. coli*. We confirmed that R90 in clones was randomly replaced with other amino acids by sequence analysis (Fig. 1).

To screen the functional mutTNFs, the binding affinities of mutTNF-R90Xs for anti-human TNF-α neutralization antibody were measured using culture supernatant (Fig. 2). As a result, mutTNF-R90R, R90P, and R90K showed significant binding affinity for the anti-TNF-α neutralization antibody. Next, cytotoxicity of mutTNF-R90Xs against L-M cells was also evaluated using culture supernatant (Fig. 3). As a result, mutTNF-R90R, R90P, and R90K showed significant cytotoxi-

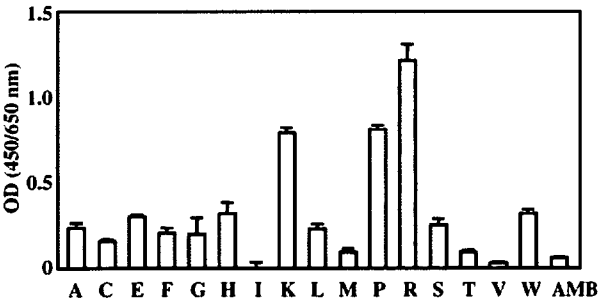

Fig. 2. Selection of clones by ELISA using anti-TNF neutralizing antibody. The reactivity of mutTNF-R90X with anti-TNF antibody was quantified by ELISA using culture supernatant of *E. coli* cells carrying the phagemid vector encoding mutTNF-R90X. Anti-TNF antibody was used as the capturing antibody, and bound mutTNF-R90X was detected with a biotinylated anti-TNF polyclonal antibody followed by addition of HRP-conjugated avidine and substrate reaction. Then the OD (450–655 nm) was measured. Each value represents the mean±SD.

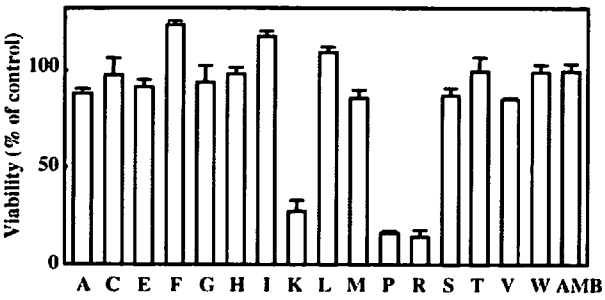

Fig. 3. Selection of clones by cytotoxicity assay using L-M cells. The cytotoxicity of mutTNF-R90X was assessed on L-M cells using culture supernatant of *E. coli* cells carrying the phagemid vector encoding mutTNF-R90X. L-M cells (3×10^4 cells/well) treated with actinomycin D were incubated with mutTNF-R90X for 24 h, and viabilities were assessed by methylene blue assay.

city to L-M cells. Other mutTNF-R90Xs have almost no affinity for anti-TNF-α antibody or show cytotoxicity. These results indicate that, as was expected, amino acid residue 90 should be lysine, arginine, or proline to retain its bioactivity and conformation.

3.2. Characterization of purified mutTNF-R90, P90, and K90

To assess their properties in detail, recombinant mutTNF-R90R, R90P, and R90K proteins were purified, and used in a binding analysis for TNF receptors, TNFR1 and TNFR2. As the result of gel filtration chromatography (GFC), the three mutTNF recombinant proteins exhibited the same retention time, indicating that they formed homotrimers (data not shown). Bioactivity of the three mutTNFs via mouse TNFR1 was confirmed using a cytotoxicity assay in L-M cells. As we reported previously, the cytotoxicity of mutTNF-R90P was almost the same as that of human wtTNF, while mutTNF-R90K was 3-fold higher and mutTNF-R90R was 5-fold higher (Fig. 4). Bioactivity of these mutTNFs via human TNFR1 was also assessed in HEp-2 cells. The cytotoxicity of mutTNF-R90P was the same as that of wtTNF. Interestingly, mutTNF-R90K and R90R exhibited 10-fold higher cytotoxicity than wtTNF (Fig. 5). Finally, bioactivity via human TNFR2 was assessed on GM-CSF production from PC60-hTNFR2 cells (human TNFR2 transfected PC60 cells). All three mutTNFs showed 2-fold higher bioactivity via TNFR2 than wtTNF (Fig. 6). These results indicate that mutTNF-R90R and R90K can stimulate TNFR1 more selectively than wtTNF.

3.3. Kinetics of mutTNFs on TNFR1 and TNFR2 affinity

The increase in affinity for TNF receptors may be one of the factors that contribute to the bioactivity enhancement. Therefore, we measured the affinities of mutTNFs for TNFR1 and TNFR2 using surface plasmon resonance (BIAcore). By comparison of the dissociation constants (KD) of mutTNFs against TNFR1, the affinities of mutTNF-R90K and R90P were 2 to 3-fold higher than wtTNF (Table 1). The affinity of mutTNF-R90P, however, was half that of wtTNF. Thus, the

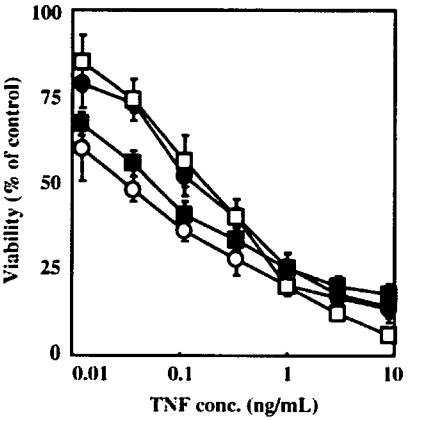

	EC50 (ng/mL)
□ wtTNF	0.17
■ mutTNF-R90K	0.05
○ mutTNF-R90R	0.03
● mutTNF-R90P	0.14

Fig. 4. Cytotoxicity of mutTNFs against L-M cells. The bioactivity of mutTNF via mouse TNFR1 was measured by the cytotoxicity assay against L-M cells in the presence of actinomycin D. Each value represents the mean±SD. The EC_{50} shows the concentration of TNF required to inhibit L-M cell viability by 50%.

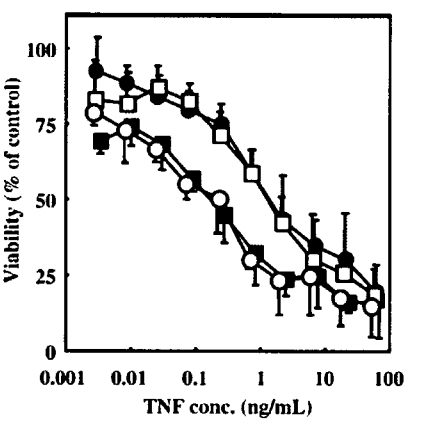

	EC50 (ng/mL)
□ wtTNF	1.30
■ mutTNF-R90K	0.17
○ mutTNF-R90R	0.15
● mutTNF-R90P	1.40

Fig. 5. Cytotoxicity of mutTNFs against HEp-2 cells. The bioactivity of mutTNF via human TNFR1 was measured by a cytotoxicity assay against HEp-2 cells in the presence of cycloheximide. HEp-2 cells (4×10^4 cells/well) were incubated with mutTNFs for 18 h, and their viabilities were assessed by methylene blue assay. Each value represents the mean±SD. The EC_{50} shows the concentration of TNF required to inhibit HEp-2 cell viability by 50%.

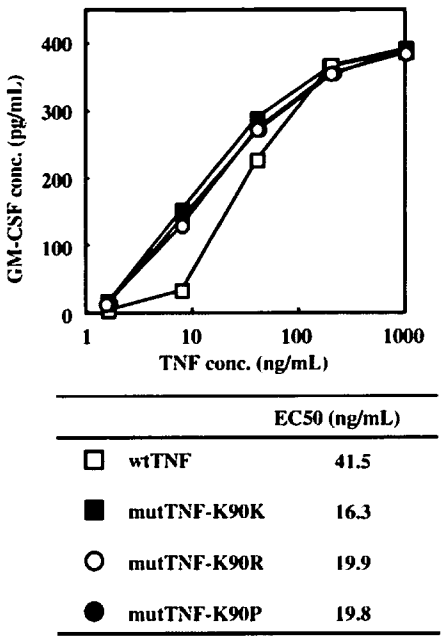

Fig. 6. Induction of GM-CSF by mutTNFs. PC60 cells transfected human TNFR2 were incubated with mutTNFs and IL-1β (2 ng/mL). After 24 h, TNFR2-mediated induction of GM-CSF was assayed by ELISA. Each value represents the mean±SD. The EC_{50} is given as the concentration of TNF-α required to induce secretion of 200 pg/mL GM-CSF.

lower bioactivity of mutTNF-R90P via TNFR1 may be due to weaker affinity for TNFR1. On the other hand, affinities of the three mutTNFs for TNFR2 were 1.2- to 1.5-fold higher than that of wtTNF (Table 2). These results suggest that replacement of amino acid residue 90 in mutTNF does not affect the affinity for TNFR2, while arginine or lysine substitution at amino acid residue 90 is better than proline for TNFR1 binding.

4. Discussion

Although systemic administration of TNF-α is limited due to its severe side effects, TNF exerts beneficial anti-tumor effects as an enhancer of tumor vascular permeability in combination cancer chemotherapy [8–10]. Therefore, the creation of an artificial mutTNF with remarkable bioactivity and in vivo stability will be important to generate a more effective cancer chemotherapy. We have previously created lysine-deficient mutTNFs, mutTNF-R90 and P90, which showed high bioactivity and in vivo stability and are suitable for site-specific mono-PEGylation [18]. We have also reported that these lysine-deficient mutTNFs show the same or higher bioactivities than wtTNF and that mono-PEGylated mutTNFs exhibit increased anti-tumor therapeutic potential. In this study, we attempted to create a new mutTNF that has more bioactivity and a tighter binding affinity when compared to mutTNF-R90 and P90. We also evaluated the role of amino acid residue 90 in bioactivity and receptor binding capacity.

Table 1
Kinetic parameters of mutant TNF-αs (TNF receptor 1)

	Ka[a] (10^5)(1/Ms)	Kd[b] (10^{-3})(1/s)	KD[c] (10^{-9})(M)	Relative[d] (%)
Human wtTNF	5.4	1.2	2.3	100
mutTNF-R90K	13.4	1.1	0.8	285
mutTNF-R90P	4.0	2.1	5.2	44
mutTNF-R90R	12.1	1.4	1.2	191

Kinetic parameters were determined from equilibrium binding using BIA evaluation 3.0 program.
[a] Association rate constant.
[b] Dissociation rate constant.
[c] Equilibrium dissociation constant.
[d] Relative values for the KD were calculated from the KD (mutants)/KD (wtTNF)×100.

Table 2
Kinetic parameters of mutant TNF-αs (TNF receptor 2)

	Ka[a] (10^6) (1/Ms)	Kd[b] (10^{-4}) (1/s)	KD[c] (10^{-10}) (M)	Relative[d] (%)
Human wtTNF	3.7	10.1	2.7	100
mutTNF-R90K	5.1	10.7	2.1	129
mutTNF-R90P	5.1	11.3	2.2	122
mutTNF-R90R	5.2	9.4	1.8	148

Kinetic parameters were determined from equilibrium binding using BIA evaluation 3.0 program.
[a] Association rate constant.
[b] Dissociation rate constant.
[c] Equilibrium dissociation constant.
[d] Relative values for the KD were calculated from the KD (mutants)/KD (wtTNF)×100.

We constructed a phage library that expresses mutTNF-R90 variants in which R90 is replaced with other amino acids and measured their affinities for anti-TNF-α and their bioactivities using culture supernatant of *E. coli*. Only mutTNF-R90X in which amino acid residue 90 was replaced with lysine, arginine, or proline exhibited affinity for anti-TNF-α and bioactivity. Therefore, it is suggested that proline, arginine and lysine at position 90 are important to retain the bioactivity of TNF-α. As described previously, K90 in wtTNF forms a hydrogen bond with E135 in TNFR1 and contributes to stabilizing the loop structure that contains residues 84 to 89, which is the receptor binding region. In the mutTNF-R90R, R90 also likely forms a hydrogen bond with E135 and perhaps contributes to stabilizing the loop structure. The basic amino acid substitution mutTNF-R90H had no bioactivity nor binding affinity. These results suggest that general replacement of R90 with a basic amino acid is not always essential for bioactivity and binding affinity to the TNF receptor. Moreover, the steric hindrance of an amino acid residue is as important as electric charge.

Lysine residues in proteins are generally believed to be important amino acids for retaining three-dimensional structure and for receptor affinity and bioactivity. In the case of TNF-α, X-ray structure analysis revealed that K11 and K98 are important for retaining protein structure and homotrimerization [20]. However, the importance of other lysine residues (K65, 90, 112, 128) has not been discussed. The only report with regard to K90 demonstrated that replacement of K90 with alanine reduced the bioactivity to half of wtTNF [21]. Our results indicate that amino acid position 90 of TNF-α is important for homotrimer formation and bioactivity.

We measured the bioactivities and affinities of mutTNF-R90R, R90K and R90P for TNF receptors. mutTNF-R90R and mutTNF-R90K demonstrated 10-fold higher cytotoxicity levels in HEp-2 cells than wtTNF. The cytotoxicity level of mutTNF-R90P was almost the same as wtTNF. Indeed, affinities of mutTNF-R90R and -R90K for TNFR1 were 2 to 3-fold higher than wtTNF, while that of mutTNF-R90P was half that of wtTNF. Thus R90 and K90 contribute to the stable formation of the TNF/TNFR1 complex, and this may be one of the factors causing increased bioactivity. On the other hand, TNFR2-dependent bioactivities of the three mutants almost doubled that of wtTNF. Affinities of the three mutants for TNFR2 were also 1.2 to 1.5 stronger that that of wtTNF. These results indicate that arginine or lysine in amino acid position 90 is necessary for mutTNFs to obtain superior bioactivity and affinity for TNFR1, but less so for TNFR2. A previous study showed that the loop structure mutant TNF S86T had TNFR1-selectivity [22]. The interaction site of this loop structure with TNFR1 is predicted to be different than with TNFR2. The lower affinity of mutTNF-R90P for TNFR1 (as compared with mutTNF-R90K or-R90R) is thought to be caused by the difference in loop structure stabilization. The hydrogen bond formed between the basic amino acid (K90 or R90) and E135 creates a more stable loop than one stabilized by the hydrophobic bond between P90 and L83. Interestingly, in the lysine-deficient mutTNF that we previously created, K90 was replaced with proline [19]. This result indicates that the loop structure formed by the hydrophobic interaction of P90 with L83 is very important to protein folding and homotrimer formation.

In this study, we created mutTNFs that substitute other amino acids in the K90 position and evaluated their bioactivities and binding affinities. The determination of the functional domain of TNF has been attempted by creating mutant TNFs like these, however, there are few reports that detailed the role of one amino acid in TNF-α. Our data demonstrate that amino acid position 90 is important for TNF bioactivity and that replacement with other amino acids will be an effective strategy to increase the bioactivity of TNF-α. In the near future, the accumulation of information about the structure–activity relationship of TNF-α using mutant TNFs will enable the generation of a super-agonist that has optimized bioactivity.

Acknowledgements

This study was supported by a Grant-in-Aid for Scientific Research (No. 17016084 and 17689008, 17790135, 18015055, 18659047) from the Ministry of Education, Culture, Sports, Science and Technology of Japan, a Health and Labor Sciences Research Grant from the Ministry of Health, Labor and Welfare of Japan, Takeda Scientific Foundation and Research Fellowships for Young Scientists.

References

[1] E.A. Carswell, L.J. Old, R.L. Kassel, S. Green, N. Fiore, B. Williamson, An endotoxin-induced serum factor that causes necrosis of tumors, Proc. Natl. Acad. Sci. U. S. A. 72 (1975) 3666–3670.

[2] E.A. Havell, W. Fiers, R.J. North, The antitumor function of tumor necrosis factor (TNF), I. Therapeutic action of TNF against an established murine sarcoma is indirect, immunologically dependent, and limited by severe toxicity, J. Exp. Med. 167 (1988) 1067–1085.

[3] L. Helson, C. Helson, S. Green, Effects of murine tumor necrosis factor on heterotransplanted human tumors, Exp. Cell Biol. 47 (1979) 53–60.

[4] W.L. Furman, D. Strother, K. McClain, B. Bell, B. Leventhal, C.B. Pratt, Phase I clinical trial of recombinant human tumor necrosis factor in children with refractory solid tumors: a Pediatric Oncology Group study, J. Clin. Oncol. 11 (1993) 2205–2210.

[5] K. Kimura, T. Taguchi, I. Urushizaki, R. Ohno, O. Abe, H. Furue, T. Hattori, H. Ichihashi, K. Inoguchi, H. Majima, Phase I study of recombinant human tumor necrosis factor, Cancer Chemother. Pharmacol. 20 (1987) 223–239.

[6] T. Moritz, N. Niederle, J. Baumann, D. May, E. Kurschel, R. Osieka, J. Kempeni, E. Schlick, C.G. Schmidt, Phase I study of recombinant human tumor necrosis factor alpha in advanced malignant disease, Cancer Immunol. Immunother. 29 (1989) 144–150.

[7] J. Skillings, R. Wierzbicki, E. Eisenhauer, P. Venner, F. Letendre, D. Stewart, B. Weinerman, A phase II study of recombinant tumor necrosis factor in renal cell carcinoma: a study of the National Cancer Institute of Canada Clinical Trials Group, J. Immunother. 11 (1992) 67–70.

[8] A.M. Eggermont, H. Schraffordt Koops, D. Lienard, B.B. Kroon, A.N. van Geel, H.J. Hoekstra, F.J. Lejeune, Isolated limb perfusion with high-dose tumor necrosis factor-alpha in combination with interferon-gamma and melphalan for nonresectable extremity soft tissue sarcomas: a multicenter trial, J. Clin. Oncol. 14 (1996) 2653–2665.

[9] D. Lienard, P. Ewalenko, J.J. Delmotte, N. Renard, F.J. Lejeune, High-dose recombinant tumor necrosis factor alpha in combination with interferon gamma and melphalan in isolation perfusion of the limbs for melanoma and sarcoma, J. Clin. Oncol. 10 (1992) 52–60.

[10] F.J. Lejeune, Clinical use of TNF revisited: improving penetration of anti-cancer agents by increasing vascular permeability, J. Clin. Invest. 110 (2002) 433–435.

[11] F.J. Lejeune, C. Ruegg, D. Lienard, Clinical applications of TNF-alpha in cancer, Curr. Opin. Immunol. 10 (1998) 573–580.

[12] P. Bailon, A. Palleroni, C.A. Schaffer, C.L. Spence, W.J. Fung, J.E. Porter, G.K. Ehrlich, W. Pan, Z.X. Xu, M.W. Modi, A. Farid, W. Berthold, M. Graves, Rational design of a potent, long-lasting form of interferon: a 40 kDa branched polyethylene glycol-conjugated interferon alpha-2a for the treatment of hepatitis C, Bioconjug. Chem. 12 (2001) 195–202.

[13] H. Kamada, Y. Tsutsumi, K. Sato-Kamada, Y. Yamamoto, Y. Yoshioka, T. Okamoto, S. Nakagawa, S. Nagata, T. Mayumi, Synthesis of a poly (vinylpyrrolidone-co-dimethyl maleic anhydride) co-polymer and its application for renal drug targeting, Nat. Biotechnol. 21 (2003) 399–404.

[14] H. Kamada, Y. Tsutsumi, Y. Yamamoto, T. Kihira, Y. Kaneda, Y. Mu, H. Kodaira, S.I. Tsunoda, S. Nakagawa, T. Mayumi, Antitumor activity of tumor necrosis factor-alpha conjugated with polyvinylpyrrolidone on solid tumors in mice, Cancer Res. 60 (2000) 6416–6420.

[15] Y. Kaneda, Y. Yamamoto, H. Kamada, S. Tsunoda, Y. Tsutsumi, T. Hirano, T. Mayumi, Antitumor activity of tumor necrosis factor alpha conjugated with divinyl ether and maleic anhydride copolymer on solid tumors in mice, Cancer Res. 58 (1998) 290–295.

[16] Y. Tsutsumi, S. Tsunoda, H. Kamada, T. Kihira, Y. Kaneda, Y. Ohsugi, T. Mayumi, PEGylation of interleukin-6 effectively increases its thrombopoietic potency, Thromb. Haemost. 77 (1997) 168–173.

[17] S.P. Monkarsh, Y. Ma, A. Aglione, P. Bailon, D. Ciolek, B. DeBarbieri, M.C. Graves, K. Hollfelder, H. Michel, A. Palleroni, J.E. Porter, E. Russoman, S. Roy, Y.C. Pan, Positional isomers of monopegylated interferon alpha-2a: isolation, characterization, and biological activity, Anal. Biochem. 247 (1997) 434–440.

[18] H. Shibata, Y. Yoshioka, S. Ikemizu, K. Kobayashi, Y. Yamamoto, Y. Mukai, T. Okamoto, M. Taniai, M. Kawamura, Y. Abe, S. Nakagawa, T. Hayakawa, S. Nagata, Y. Yamagata, T. Mayumi, H. Kamada, Y. Tsutsumi, Functionalization of tumor necrosis factor-alpha using phage display technique and PEGylation improves its antitumor therapeutic window, Clin. Cancer Res. 10 (2004) 8293–8300.

[19] Y. Yamamoto, Y. Tsutsumi, Y. Yoshioka, T. Nishibata, K. Kobayashi, T.

Okamoto, Y. Mukai, T. Shimizu, S. Nakagawa, S. Nagata, T. Mayumi, Site-specific PEGylation of a lysine-deficient TNF-alpha with full bioactivity, Nat. Biotechnol. 21 (2003) 546–552.

[20] M.J. Eck, S.R. Sprang, The structure of tumor necrosis factor-alpha at 2.6 A resolution. Implications for receptor binding, J. Biol. Chem. 264 (1989) 17595–17605.

[21] J. Yamagishi, H. Kawashima, N. Matsuo, M. Ohue, M. Yamayoshi, T. Fukui, H. Kotani, R. Furuta, K. Nakano, M. Yamada, Mutational analysis of structure–activity relationships in human tumor necrosis factor-alpha, Protein Eng. 3 (1990) 713–719.

[22] H. Loetscher, D. Stueber, D. Banner, F. Mackay, W. Lesslauer, Human tumor necrosis factor alpha (TNF alpha) mutants with exclusive specificity for the 55-kDa or 75-kDa TNF receptors, J. Biol. Chem. 268 (1993) 26350–26357.

Department of Biopharmaceutics[1], Graduate School of Pharmaceutical Sciences, Osaka University, Laboratory of Pharmaceutical Proteomics (LPP)[2], National Institute of Biomedical Innovation (NiBio), Frontier Research Center[3], Osaka University (FRC), Osaka, Japan

Creation of a novel cell penetrating peptide, using a random 18mer peptides library

T. Nomura[1,2], M. Kawamura[1], H. Shibata[1,2,3], Y. Abe[1,2], A. Ohkawa[1,2], Y. Mukai[1,2], T. Sugita[1,2], S. Imai[1,2], K. Nagano[1,2], T. Okamoto[1], Y. Tsutsumi[1,2], H. Kamada[2], S. Nakagawa[1,3], S. Tsunoda[2]

Received December 1, 2006, accepted December 18, 2006

Haruhiko Kamada, Ph.D, Laboratory of Pharmaceutical Proteomics, National Institute of Biomedical Innovation (NiBio), 7-6-8 Saito-Asagi, Ibaraki, Osaka 567-0085, Japan
kamada@nibio.go.jp

Pharmazie 62: 569–573 (2007) *doi: 10.1691/ph.2007.8.6278*

Cell penetrating peptides (CPPs) have drawn attention as carriers for intracellular drug delivery. It is commonly believed that TAT peptide is the best carrier among the existing CPPs due to its high translocational activity. Despite considerable research, the cellular uptake mechanism of TAT peptide remains unclear. Additionally, the transduction efficiency of TAT peptide is insufficient for use in intracellular therapy. In this study, we attempted to identify novel CPPs from a random 18mer peptide library using a phage display system. To isolate novel CPPs more effectively, PSIF (protein synthesis inhibition factor) was used with the screening system. Consequently, we isolated 7 novel CPPs from the library and determined by flow cytometry and confocal laser microscopy that these CPPs were taken up into cells. Once the cellular uptake pathway of these CPPs has been determined, it may be possible to use them for intracellular therapy.

1. Introduction

With the progress of proteomics technology over the last few years, many disease-related proteins have been discovered (Kuncl et al. 2002; Lambrechts et al. 2003; St Croix et al. 2000). Many of these proteins reside within the cell. To therapeutically modulate disease-related-proteins, effective methods are needed to deliver other regulatory proteins into cells. Recently, cell penetrating peptides (CPPs) have received considerable attention in this regard (Derossi et al. 1998; Wadia and Dowdy 2002). Examples of CPPs include short peptide segments derived from HIV-1 TAT (Frankel and Pabo 1988; Green and Loewenstein 1988) (13 a.a), *Drosophila* Antennapedia homeodomain proteins (Joliot et al. 1991) (16 a.a), and *Herpes simplex* virus VP22 (Elliott and O'Hare 1997) (17 a.a) are examples of CPP peptides. Because CPPs can translocate various molecules (e.g., peptides, proteins, plasmids, and nucleotides (Astriab-Fisher et al. 2000)) into the cells, CPPs are expected to be useful as carriers for intracellular drug delivery. Of the existing CPPs, TAT peptide is the most effective carrier, and has been used as a carrier to deliver p53 protein for tumor suppression (Li et al. 2002). There are several factors, however, that limit the therapeutic use of CPPs. Firstly, although the mechanism of translocation is thought to be mediated via an endocytic pathway, the precise mechanism of how TAT peptide translocates across the membrane and escapes from the endosome remains unclear. Secondly, the transduction efficiency of TAT peptide is too low to effectively modulate disease-related-proteins. Therefore, for intracellular therapy, novel CPPs are needed that can introduce target proteins into cells more efficiently than existing CPPs by different mechanisms.

Phage libraries expressing polypeptides, such as single-chain antibodies (Imai et al. 2006; Okamoto et al. 2004) or random peptides (Chung et al. 2002; Connor et al. 2001; Scott and Smith 1990), have been used extensively to identify specific molecules with high affinity for target ligands. In the past, novel CPPs have been developed using random peptide phage libraries and cell panning (Hou et al. 2004; Landon and Deutscher 2003; Mi et al. 2003). However, with cell panning, cell-penetrating peptides are difficult to obtain because these peptides bind to the entire cell surface. We previously developed an effective system for screening CPPs using PSIF (protein synthesis inhibition factor). PSIF, a bacteria-derived protein toxin, is non-cytotoxic extracellularly, but once incorporated into cells, it can induce cell death rapidly (Chaudhary et al. 1990; Ogata et al. 1990; Song et al. 2005). CPPs can simply be identified using PSIF-mediated cytotoxicity as an index. In this study, we attempted to create novel CPPs, with greater transduction efficiency cell-penetrating mechanisms that differ from existing CPPs, using a random peptide phage library and a screening system with PSIF.

Table 1: Amino acid sequence of 9 clones selected from random 18 mer peptide library

Clone	Sequence
1	Y A Q Y K I T T A S P G D V K T S N
2	T Y A W Q Y C Q R T G R A L P N T K
3	R K H D A M D S T R R C W P H A P C
4	H N Q R H V K N W P D G F Q R N W S
5	K E Q K N P Q K Q F S S R G P A P N
6	Y P R Y K L Q D T V Q D R L R H R H
7	P K D A Q A S Y T P N N F N L S T T
8	M R Q P K P D T S N Y K D R V K S S
9	M F K G A F T Q Y H S T H E S T E N

2. Investigations, results and discussion

In a first step, a random 18mer peptide phage library was constructed in consideration of cell membrane thickness and the length of existing CPPs. We confirmed that the diversity of the library was 2.0×10^6 CFU, and 9 randomly selected clones consisted of different amino acids as shown by sequence analysis (Table 1). Cell panning was then performed using this library to select clones binding to A431 cells. We evaluated the efficacy of cell panning by calculating the ratio of input to output phage. With successive panning rounds, the ratio of output phage to input phage was increased by approximately 72-fold (Fig. 1). This data suggests that the number of peptide-displaying phages bound to A431 cells was increased. Phagemids of the phage clones selected by cell panning were collected, and the genes encoding peptides were recombined into the PSIF fusion peptide expression vector.

PSIF, which is non-toxic outside the cell, is highly cytotoxic: it inhibits protein synthesis even when only a few molecules are released into the cytosol. PSIF fusion peptides were produced in culture medium of *E. coli*, and applied to A431 cells. We examined the transduction efficacy of peptides into cytoplasm as an index of cytotoxicity of peptide-PSIF fusion protein (Fig. 2). The viability of cells treated with PSIF fusion peptide was calculated by setting

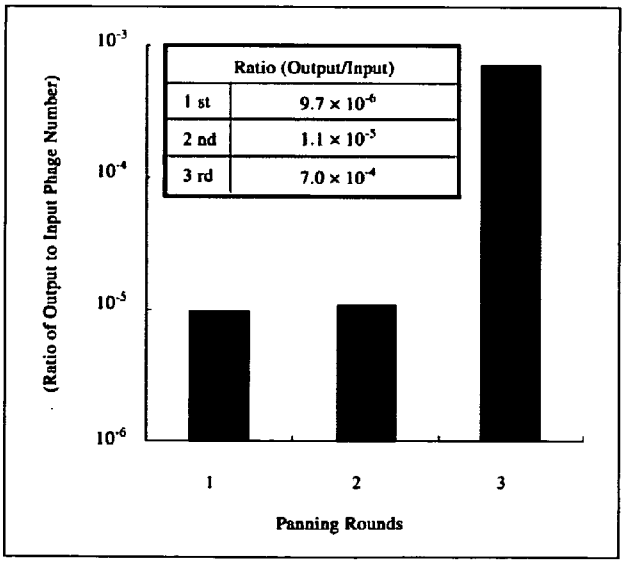

Fig. 1: Selection of binding and internalized phage clones by panning to A431. Phage clones binding to A431 cells with high affinity were collected. The ratio (output phage/input phage) in 3 rounds of panning was calculate. The number of phage clones binding to A431 cells increased with successive rounds of panning

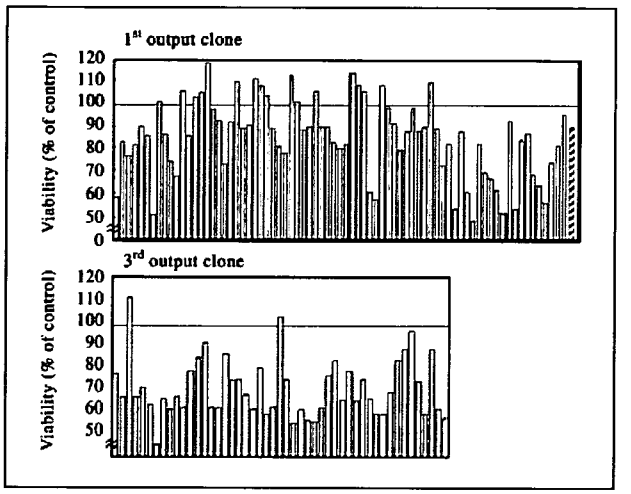

Fig. 2: Cytotoxic activity of randomly selected clones from a random 18mer peptide library. Phage clones were collected after 1 or 3 rounds of panning and genes encoding peptides were recombined with PSIF expression vector. Cytotoxicity mediated by PSIF fusion peptide from randomly selected clones was measured by MTT assay in A431 cells. The viability of A431 cells treated with PSIF fusion TAT peptide was 100%. Clones: (open bar), TAT13: (filled bar)

the viability treated with PSIF fusion TAT peptide at 100%. The rate of clones with viability less than 80% in the first panning output was 16 out of 75 clones (21.3%), and in the third panning it was 28 out of 49 clones (57.1%). We selected 8 clones that introduced PSIF most effectively into the cell, and assessed their cytotoxicity for reproducibility (Fig. 3). The cellular uptake of all PSIF fusion peptides was greater than that of TAT peptide, and their amino acid sequences were analyzed. We then analyzed the phagemid sequences and identified 7 peptides that consisted of different amino acids (Table 2). Existing CPPs consist mainly of basic amino acids and are positively-charged so that they interact with the negatively-charged surface of the cell membrane (Tyagi et al. 2001; Vives et al. 1997; Ziegler and Seelig 2004), and this interaction is important for translocation. Interestingly, 7 peptides were mainly composed of hydrophobic amino acids and contained very few basic amino acids such as lysine and arginine, and were not positively-charged. It has also been reported that cell surface binding of cationic TAT

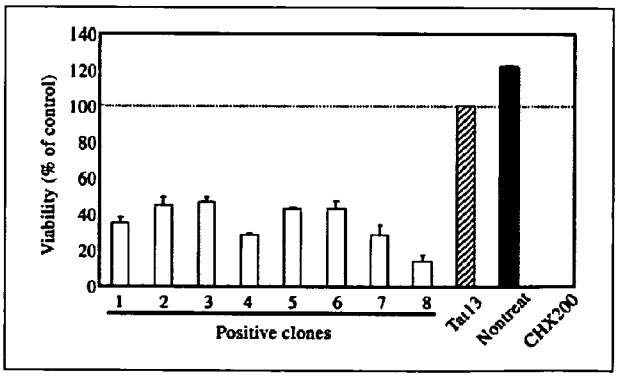

Fig. 3: Cytotoxic activity of positive clones. Positive clones were evaluated with TAT13-PSIF. Eight clones showing strong cytotoxic activity were identified and cytotoxic activity was measured by MTT assay. The viability of A431 cells treated with PSIF fusion TAT peptide was 100%, and the viability of cells treated with 200 mg/ml cycloheximide (CHX200) as a positive control was 0%. Clones: (open bar), TAT13: (hatched bar), Nontreat: (filled bar)

Table 2: Amino acid sequence of positive clones selected by screening with PSIF from random 18 mer peptide library

Clone	Sequence
1	S G E H T N G P S K T S V R W V W D
2	S M T T M E F G H S M I T P Y K I D
3	Q D G G T W H L V A Y C A K S H R Y
4	M S D P N M N P G T L G S S H I L W
5	S P G N Q S T G V I G T P S F S N H
6/7	S S G A N Y F F N A I Y D F L S N F
8	G T S R A N S Y D N L L S E T L T Q
Tat13	G R K K R R Q R R R P P Q
An-tenna-pedia	R Q I K I W F Q N R R M K W K K
VP22	N A K T R R H E R R R K L A I E R

peptide is inhibited by pentosan polysulfate (Rusnati et al. 2001), or heparin (Rusnati et al. 1999). Thus, these peptides might be taken up by different pathways than existing CPPs.

Flow cytometric analysis was performed on the 7 FITC-labeled peptides to evaluate transduction efficacy. The penetration of clones 3 and 6/7 in A431 cells was more than 90% greater than that of FITC-labeled TAT peptide (Fig. 4a). In HeLa cells, clone 6/7 was taken up more effectively than TAT peptides (Fig. 4b). Flow cytometry showed that FITC-labeled clone3 was taken up most effectively in A431 and confocal laser scanning microscopy showed was translocated in A431 cells to the same degree as TAT peptide (Fig. 5). However, results from flow cytometric analysis using FITC-labeled peptides differed from those of the MTT assay using PSIF fusion peptides. With respect to TAT peptide, the 7 peptides fused with PSIF as a cargo molecule were introduced more effectively than peptides fused with low-molecular-weight compound like

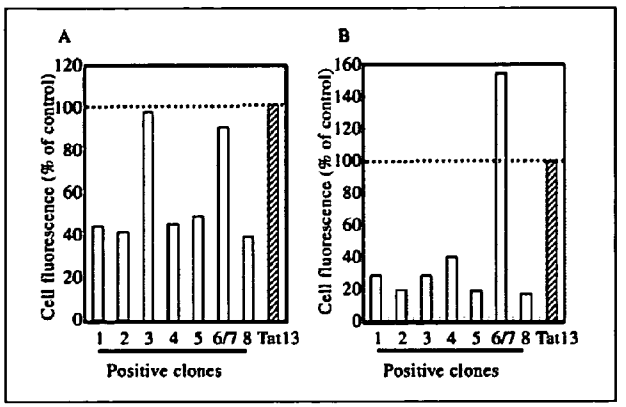

Fig. 4: Cellular uptake of positive clones in the cells. Positive clones were evaluated with FITC-labeled Tat13. A431 cells (A) or HeLa cells (B) were incubated with edium containing FITC-labeled peptide (1 mM) for 3 h. Intracellular translocated peptides were quantified with a a FACScan flow cytometer. Samples were treated with 0.25% trypsin before FACS analysis. The viability of A431 cells treated with PSIF fusion TAT peptide was 100%. Clones: (open bar), TAT13: (hatched bar)

FITC. These data suggest that the molecular weight of the cargo molecule has a considerable effect on the transduction efficiency of CPPs, depending on the characteristics and mechanism of penetration of the CPPs.

In this study, we used a random 18mer peptide library with a PSIF screening system to successfully create novel CPPs that efficiently introduced proteins into cells. We are now investigating the mechanism of penetration of these peptides in studies using inhibitors of cellular uptake pathways. We are also attempting to clarify the relationship between molecular weight of cargo molecules and transduction efficiency with several CPPs. Our data may contribute to the development of intracellular therapy with disease-related proteins.

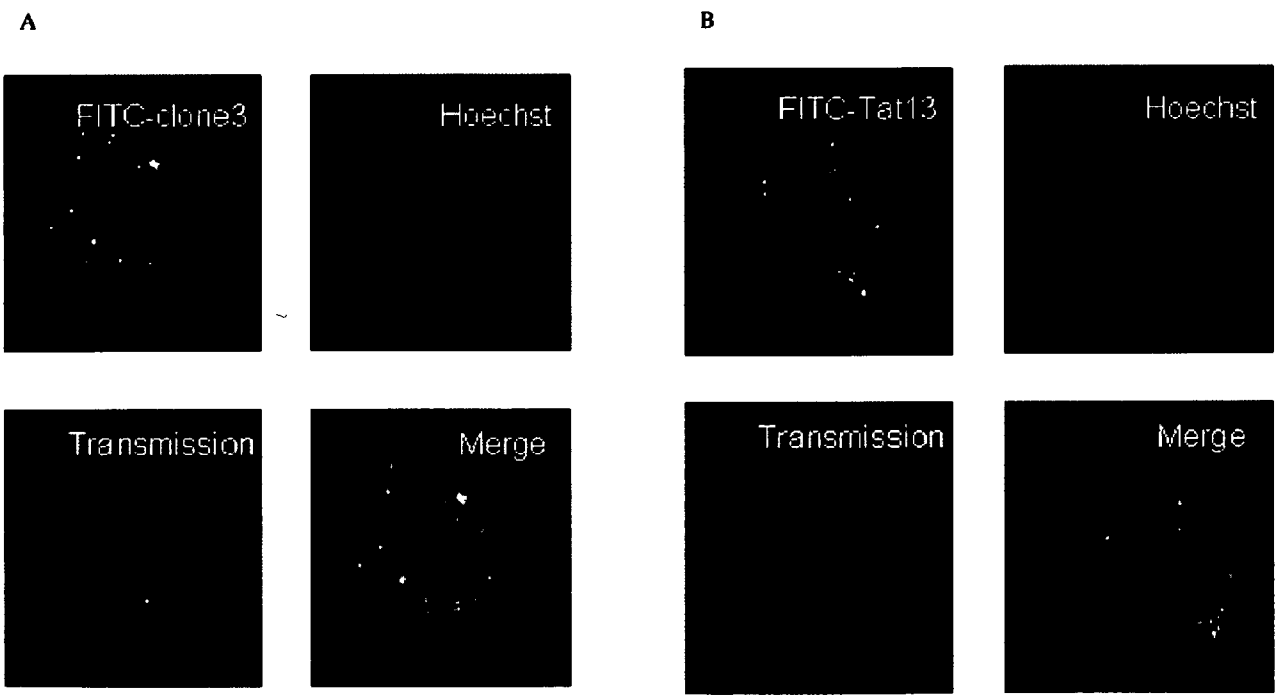

Fig. 5: Intracellular distribution of clone3 in living cells. A431 cells were cultured with FITC-labeled clone3 (A) or TAT peptide (B) for 3 h. Cells were washed and nuclei were stained with Hoechst 33342. Cells were examined by confocal laser microscopy

3. Experimental

3.1. Construction of gene fragment library coding random 18mer amino acids peptide

Gene fragments encoding random 18mer amino acid peptides were produced with Klenow fragment and the following primers: P-oligo1 (5′-GATTACGCCAAGCTTTGGAGCCTTTTTTTTGGAGATTTTCAACGTGAAAAAATTATTATTCGCAATTCCTTTAGTTGTTCCTTTCTATGCGGCCCAGCCGGCCATGGCC-3′), P-oligo4(5′-CGGCGCACCTGCGGCCGCSNNSNNSNNSNNSNNSNNSNNSNNSNNSNNSNNSNNSNNSNNSNNSNNSNNGGCCATGGCCGGCTGGGCCGCATAGAA-3′).

To anneal the primers, 25 pmol each of P-oligo1 and P-oligo4 were mixed with 10 × Klenow buffer and incubated at 96 °C for 10 min, 70 °C for 5 min, and 16 °C for 10 min. Klenow fragment (TOYOBO) and 10 mM dNTP were then added to the reaction mixture and incubation was continued at 37 °C for 1 h. The purified sample was extracted from agarose gel using a QIAquick Gel Extraction Kit (QIAGEN). Gene fragments were then amplified by PCR. PCR reactions were cycled 35 times at 96 °C for 1 min, 65 °C for 1 min, 68 °C for 1 min, using pCANTAB HindIII (5′-GGAAACAGCTATGACCATGATTACGCCAAG-3′), and NotI extension (5′-GTAAATGAATTTTCTGTATGAGG-3′) as primers. The gene library and pCANTAB5E phagemid vector were digested with Hind III and Not I, and ligated with T4 ligase to display random 18mer amino acid peptides on the phage surface as fusion proteins with gene 3 protein. The phage library was prepared as previously described. Sequence analysis of randomly selected clones was performed.

3.2. Cell panning

A431 cells (epidermoid carcinoma, human) were maintained in Dulbecco's modified Eagle's medium supplemented with 10% fetal bovine serum (FBS) and 1% antibiotics. A431 cells (1.0×10^6 cells/2 ml/well) were seeded in 6-well plates and grown for 24 h. The wells were washed three times with PBS, and then incubated at 37 °C for 2 h with 2 ml/well Opti-MEM®I Reduced-Serum Medium (Invitrogen™ Life Techologies) containing 2% BSA. Medium was removed from each well, and the cells were incubated at 37 °C for 2 h with the purified phage library ready blocked with Opti-MEM containing 2% BSA. After washing the wells with PBS 20 times, the bound phages were eluted by incubating the wells with 100 mM HCl solution at 4 °C for 10 min. Eluted phages were immediately neutralized with 1 M Tris-HCl buffer pH 8.0 and were recovered as output phages. For the next panning, the eluted solution was added to log phase *E. coli* TG1 cells (Stratagene). The ratio of output phage to input phage was calculated to determine the effects of cell panning. Input phage and output phage were diluted in 2YT medium containing 50 μg/ml ampicillin and 2% glucose, and added to log phase *E. coli* TG1 cells. After incubation at 37 °C for 1 h, *E. coli* solution was seeded on LB (50 μg/ml ampicillin and 2% glucose) plates, and the number of colonies formed were counted.

3.3. Recombination to PSIF-expression vector

Protein synthesis inhibitory factor (PSIF, PE fragment) is an approximately 40kD fragment of the bacterial exotoxin (GenBank Accession No. K01397) derived from *Pseudomonas aeruginosa* (ATCC strain No. 29260). PSIF lacks its cell binding domain, and is the truncated form of *Pseudomonas aeruginosa* exotoxin, which is a non-toxic protein outside of the cell. One (Dr. Tsunoda) of us cloned the cDNA for PSIF from *Pseudomonas aeruginosa*, Migula by PCR using the primer set 5′-GAT GAT CGA TCg cgg ccg caG GTG CGC CGG TGC CGT ATC CGG ATC CGC TGG AAC CGC GTG CCG CAg act aca aag acg acg acg aca aaC CCG AGG GCG GCA GCC TGG CCG CGC TGA CC-3′ and 5′-GAT CGA TCG ATC act agt CTA cag ttc gtc ttt CTT CAG GTC CTC GCG CGG CGG TTT GCC GGG-3′. The fusion protein, denoted peptide-PSIF, consisted of peptide at the N-terminus and a PSIF at the C-terminus. First, the peptide gene containing phagemid vectors were recovered with QIAprep® Miniprep Kit (QIAGEN) and digested with HindIII and NotI. The peptide gene fragments encoding random 18mer amino acids were then subcloned into PSIF Expression Vector, which is modified from pCANTAB-5E.

3.4. Cytotoxicity assay by PSIF-fusion peptide

PSIF display phagemid was was transfected into TG1 cells, and individual TG1 clones were selected and grown at 37 °C in 96-well plates. Supernatants of TG1 cells were prepared for MTT assay. After seeding of A431 cells treated with 10 μg/ml cycloheximide at 2.0×10^4 cells/50 μl/well, 35 μL of Opti-MEM and 5 μl of supernatant were added to each well. After incubation at 37 °C for 24 h, 10 μL of 5 mg/ml MTT (3-(4,5-dimethylthiazol-2yl)-2,5-diphenyltetrazolium bromide) solution was added. MTT assays were carried out according to the manufacturer's protocol.

3.5. Flow cytometry

A431 and Hela cells (2.0×10^5 cells/well in 12-well plates) were grown for 24 h and incubated with each FITC-labeled clone peptide or TAT peptide at 37 °C for 3 h. The cells were washed twice with PBS and once with PBS/EDTA, and then treated with 0.25% trypsin for 10 min. The cells were collected, and fixed with PBS (500 μl/well) containing 1% PFA. The fluorescence intensities of the samples were measured with a FACS calibur (Becton Dickinson) detector.

3.6. Confocal laser scanning microscopy

Confocal laser scanning microscopy was performed using a Leica TCS SP2 (Leica). A431 cells were seeded at 2.25×10^4 cells/well in 4-well chamber slide glasses. After overnight incubation, cells were washed once with phenol red-free DMEM containing 10% FBC and 1% antibiotics. Each peptide (TAT peptide and clone3) and nuclear stain marker Hoechst33342 (molecular probes) were added at a concentration of 100 ng/ml in 500 μl of serum-free Opti-MEM), and then incubated at 37 °C for 3 h. The cells were subsequently washed three times and then analyzed.

Acknowledgements: This study was supported in part by Grants-in-Aid for Scientific Research (No. 17689008, 17016084, 17790135, 18015055, 18659047) from the Ministry of Education, Culture, Sports, Science and Technology of Japan, in part by Health and Labor Sciences Research Grant from the Ministry of Health, Labor and Welfare of Japan, in part by Health Sciences Research Grants for Research on Health Sciences focusing on Drug Innovation from the Japan Health Sciences Foundation, in part by Takeda Science Foundation, in part by Industrial Technology Research Grant Program (No. 03A47016a) from New Energy and Industrial Technology Development Organization (NEDO), and in part by JSPS Research Fellowships for Young Scientists (No. 08476, 08841, 09131) from the Japan Society for the Promotion of Science.

References

Astriab-Fisher A, Sergueev DS, Fisher M, Shaw BR, Juliano RL (2000) Antisense inhibition of P-glycoprotein expression using peptide-oligonucleotide conjugates. Biochem Pharmacol 60: 83–90.

Chaudhary VK, Jinno Y, FitzGerald D, Pastan I (1990) Pseudomonas exotoxin contains a specific sequence at the carboxyl terminus that is required for cytotoxicity. Proc Natl Acad Sci USA 87: 308–312.

Chung J, Park S, Kim D, Rhim J, Kim I, Choi I, Yi K, Ryu S, Suh P, Chung D, Bae Y, Shin Y (2002) Identification of antigenic peptide recognized by the anti-JL1 leukemia-specific monoclonal antibody from combinatorial peptide phage display libraries. J Cancer Res Clin Oncol 128: 641–649.

Connor CE, Norris JD, Broadwater G, Willson TM, Gottardis MM, Dewhirst MW, McDonnell DP (2001) Circumventing tamoxifen resistance in breast cancers using antiestrogens that induce unique conformational changes in the estrogen receptor. Cancer Res 61: 2917–2922.

Derossi D, Chassaing G, Prochiantz A (1998) Trojan peptides: the penetratin system for intracellular delivery. Trends Cell Biol 8: 84–87.

Elliott G, O'Hare P (1997) Intercellular trafficking and protein delivery by a herpesvirus structural protein. Cell 88: 223–233.

Frankel AD, Pabo CO (1988) Cellular uptake of the tat protein from human immunodeficiency virus. Cell 55: 1189–1193.

Green M, Loewenstein PM (1988) Autonomous functional domains of chemically synthesized human immunodeficiency virus tat trans-activator protein. Cell 55: 1179–1188.

Hou ST, Dove M, Anderson E, Zhang J, MacKenzie CR (2004) Identification of polypeptides with selective affinity to intact mouse cerebellar granule neurons from a random peptide-presenting phage library. J Neurosci Methods 138: 39–44.

Imai S, Mukai Y, Nagano K, Shibata H, Sugita T, Abe Y, Nomura T, Tsutsumi Y, Kamada H, Nakagawa S, Tsunoda S (2006) Quality enhancement of the non-immune phage scFv library to isolate effective antibodies. Biol Pharm Bull 29: 1325–1330.

Joliot A, Pernelle C, Deagostini-Bazin H, Prochiantz A (1991) Antennapedia homeobox peptide regulates neural morphogenesis. Proc Natl Acad Sci USA 88: 1864–1868.

Kuncl RW, Bilak MM, Bilak SR, Corse AM, Royal W, Becerra SP (2002) Pigment epithelium-derived factor is elevated in CSF of patients with amyotrophic lateral sclerosis. J Neurochem 81: 178–184.

Lambrechts D, Storkebaum E, Morimoto M, Del-Favero J, Desmet F, Marklund SL, Wyns S, Thijs V, Andersson J, van Marion I, Al-Chalabi A, Bornes S, Musson R, Hansen V, Beckman L, Adolfsson R, Pall HS, Prats H, Vermeire S, Rutgeerts P, Katayama S, Awata T, Leigh N, Lang-Lazdunski L, Dewerchin M, Shaw C, Moons L, Vlietinck R, Morrison KE, Robberecht W, Van Broeckhoven C, Collen D, Andersen PM, Carmeliet P (2003) VEGF is a modifier of amyotrophic lateral sclerosis in mice and humans and protects motoneurons against ischemic death. Nat Genet 34: 383–394.

Landon LA, Deutscher SL (2003) Combinatorial discovery of tumor targeting peptides using phage display. J Cell Biochem 90: 509–517.

Li Y, Rosal RV, Brandt-Rauf PW, Fine RL (2002) Correlation between hydrophobic properties and efficiency of carrier-mediated membrane transduction and apoptosis of a p53 C-terminal peptide. Biochem Biophys Res Commun 298: 439–449.

Mi Z, Lu X, Mai JC, Ng BG, Wang G, Lechman ER, Watkins SC, Rabinowich H, Robbins PD (2003) Identification of a synovial fibroblast-specific protein transduction domain for delivery of apoptotic agents to hyperplastic synovium. Mol Ther 8: 295–305.

Ogata M, Chaudhary VK, Pastan I, FitzGerald DJ (1990) Processing of Pseudomonas exotoxin by a cellular protease results in the generation of a 37,000-Da toxin fragment that is translocated to the cytosol. J Biol Chem 265: 20678–20685.

Okamoto T, Mukai Y, Yoshioka Y, Shibata H, Kawamura M, Yamamoto Y, Nakagawa S, Kamada H, Hayakawa T, Mayumi T, Tsutsumi Y (2004) Optimal construction of non-immune scFv phage display libraries from mouse bone marrow and spleen established to select specific scFvs efficiently binding to antigen. Biochem Biophys Res Commun 323: 583–591.

Rusnati M, Tulipano G, Spillmann D, Tanghetti E, Oreste P, Zoppetti G, Giacca M, Presta M (1999) Multiple interactions of HIV-I Tat protein with size-defined heparin oligosaccharides. J Biol Chem 274: 28198–28205.

Rusnati M, Urbinati C, Caputo A, Possati L, Lortat-Jacob H, Giacca M, Ribatti D, Presta M (2001) Pentosan polysulfate as an inhibitor of extracellular HIV-1 Tat. J Biol Chem 276: 22420–22425.

Scott JK, Smith GP (1990) Searching for peptide ligands with an epitope library. Science 249: 386–390.

Song S, Xue J, Fan K, Kou G, Zhou Q, Wang H, Guo Y (2005) Preparation and characterization of fusion protein truncated Pseudomonas Exotoxin A (PE38KDEL) in Escherichia coli. Protein Expr Purif 44: 52–57.

St Croix B, Rago C, Velculescu V, Traverso G, Romans KE, Montgomery E, Lal A, Riggins GJ, Lengauer C, Vogelstein B, Kinzler KW (2000) Genes expressed in human tumor endothelium. Science 289: 1197–1202.

Tyagi M, Rusnati M, Presta M, Giacca M (2001) Internalization of HIV-1 tat requires cell surface heparan sulfate proteoglycans. J Biol Chem 276: 3254–3261.

Vives E, Brodin P, Lebleu B (1997) A truncated HIV-1 Tat protein basic domain rapidly translocates through the plasma membrane and accumulates in the cell nucleus. J Biol Chem 272: 16010–16017.

Wadia JS, Dowdy SF (2002) Protein transduction technology. Curr Opin Biotechnol 13: 52–56.

Ziegler A, Seelig J (2004) Interaction of the protein transduction domain of HIV-1 TAT with heparan sulfate: binding mechanism and thermodynamic parameters. Biophys J 86: 254–263.